Roles of RCAN1 in Metabolism

Essra Aloyouni

2143506

Aloy0004

Supervised by: Professor Damien Keating

Co- supervisor: Dr Amanda Lumsden

Declaration:

I certify that this thesis does not contain material which has been accepted for the award of any degree or diploma; and to the best of my knowledge and belief it does not contain any material previously published or written by another person except where due reference is made in the text of this thesis.

Essra Aloyouni

Acknowledgment

First and foremost, I would like to thank my supervisor Professor Damien Keating and my Co-supervisor Dr. Amanda Lumsden for all their help and guidance throughout my master research project. Working with you was a great opportunity, which give me more knowledge and experience.

I would also like to give special thanks to Alyce Martin for being very supportive, helpful during my training session. This would not have been possible without her comforting words and motivation. I would also thank Keating's lab for their incorporation. Special thanks to the school of Health Science, Saudi Arabian culture mission in Australia, and Saudi ministry of higher education for their support during my studies.

I would like to express my gratitude toward my family for their encouragement and support that motivate me to work hard and complete my research.

Table of Contents

Abstract:

Obesity and type 2 diabetes are major health problems in the world. There are several risk factors for type 2 diabetes such as age, obesity, pregnancy, stress, and genetics. Approximately 90% of diabetic people with type 2 are obese or overweight. This thesis aims to develop and improve the metabolism by regulating obesity by focusing on a gene called *RCAN1*. Regulator of calcineurin 1 (RCAN1) is a gene located on chromosome 21 and primarily expressed in adipose tissue, liver, brain, heart, skeletal muscle, and pancreas. It has a well-known role as an endogenous inhibitor of the phosphatase, calcineurin, which is important for the transcription factors in the cells. RCAN1 has two main isoforms named RCAN1.1 and RCAN1.4. These isoforms result from alternate transcripts with unique promoters and first exons. RCAN1 plays essential roles in metabolism, such as regulating obesity. Unpublished data from our lab shows that RCAN1 knock out mice are protected from obesity when placed on a high fat diet, indicating that this gene controls obesity by reducing fat mass. Furthermore, mice lacking RCAN1 show enhanced activation of an adaptive thermogenesis program in white adipose tissue under high fat diet conditions. In other words, RCAN1 plays important roles in whole body thermogenesis, which increase weight loss, in a process called adipocyte 'browning'. A practical way to reduce obesity may therefore be through the use of drugs that can inhibit RCAN1. IRCA drugs (IRCA1, IRCA2, IRCA3, IRCA4, and IRCA5) have been identified as RCAN1 inhibitors.

In this project, we focused on four different aims in relation to RCAN1 and its role in obesity. First, we examined *Rcan1* expression in relation to age in white adipose tissue to see whether the expression increases with age. Second, we examined the expression of *Rcan1* in white adipose tissue in relation to diet in mice after a high fat diet compared to a normal fat diet. Third, we measured the expression of genes associated with thermogenesis in white adipose tissue in the presence or absence of Rcan1 in mice. Finally, we tested whether five RCAN1 inhibitors can affect fat storage in an adipocyte cell line RCAN1-associated metabolic phenotypes *in vitro.* This aim was approached by treating 3T3-L1 cell lines with IRCA Drugs to test the effect of them on

differentiation and after differentiation. This study found that *Rcan1* expression does not change across different ages in white adipose tissue. In addition, the data shows that *Rcan1* gene expression seems to increases in white adipose tissue after a high fat diet compared to the low fat diet. The expression of thermogenesis genes seems to decrease in wild type white adipose tissue compared to Rcan1 knockout tissue. Furthermore, we provide a novel method to regulate obesity by using IRCA drugs that inhibit the function of RCAN1 to reduce fat mas in *vitro*. All of these drugs found to have an effect of reducing fat mass on the cell line that we used by different percentage.

1. Introduction

1.1 Obesity and Type 2 Diabetes.

It is clear that obesity is a worldwide epidemic and a major cause of diabetes. From 1980 to 2014, the number of people with diabetes has increased dramatically (especially in low and middle-income countries) from 108 million to 422 million (World Health Organization [WHO], 2016). Around 90% of diabetic patients suffer from type 2 diabetes (Marchetti et al., 2008). Type 2 diabetes can increase the risk of developing cardiovascular disease, ketoacidosis, blindness, nervous system disorders and kidney complications, and therefore decreased life expectancy (American Diabetes Association., 2006). There are many benefits to understanding the cause of the disease, and how we can treat it.

Type 2 diabetes is a progressive condition caused by reduced production of insulin coupled with severe insulin resistance (Zhao et al., 2009). In healthy individuals, insulin regulates the level of glucose that can be converted into energy when needed (Saltiel and Kahn, 2001). When insulin is released into the circulation, insulin-sensing cells within tissues such as skeletal muscle, liver and fat respond by transporting glucose out of the blood and storing it. Insulin stops the liver from making new glucose by gluconeogenesis (Rahier et al., 2008). Insulin is produced by β-cells, glucose responsive cells located in the pancreas in specific areas called the islets of Langerhans. One of the major causes of type 2 diabetes is β-cell dysfunction when either less insulin is produced by β-cells or the number of β-cells is reduced (Rahier et al., 2008, Prentki and Nolan, 2006).

Prevention and even treatment of type 2 diabetes is possible by following a healthy diet, controlling body weight, not smoking, and being physically active (WHO., 2016). However, maintaining a healthy body weight is the most important factor, since obesity plays an important role in the prevalence of type 2 diabetes (Barnett and Kumar, 2009). Obesity is considers as one of the risk factors of type 2 diabetes because of increased fat mass, individuals with obesity tend to become

less sensitive to insulin, which can lead to hyperglycaemia and eventually can cause diabetes (Barnett and Kumar, 2009). Even though the connection between obesity and insulin resistance among obese subjects has been well known since the work of Rabinovitz and Zierler (1962) (Rabinowitz and Zierler, 1962), this mechanism linking obesity and insulin resistance was only recognized recently.

Due to the direct link between obesity and type 2 diabetes, investigating the factors that affect obesity may shed some light on our understanding of how diabetes develops and my lead to the discovery of more effective measures in controlling obesity and treating type 2 diabetes. A number of factors that are linked to obesity that are also risk factors for type 2 diabetes, such as genetics (Cummings and Schwartz, 2003), unhealthy diet, inactivity (Cecchini et al., 2010), age, and even social and economic status (Wang and Beydoun, 2007) have been subjects of research in the last few decades.

1.2 Challenges of studying the genetics of obesity

Based on the complexity of different genetic contributions to human metabolic disorders, it has been difficult to work out the pathway to obesity and diabetes pathogenesis. It has been challenging to understand the cause of obesity, because it is a complex disorder and it is hard to define a phenotypes or which is the best phenotype to use.

Understanding the complicated genetic map of obesity would increase our knowledge of the regulation of energy in the body, and eventually make it possible to control the complications caused by obesity through pharmacotherapeutic interventions. We have found knocking out *Rcan1* protect against obesity, which suggest that it has a key role in regulating pathways involved in obesity and type 2 diabetes. In the following section, RCAN1 will be introduced along with its possible role in metabolism, and obesity.

1.3 Regulator of Calcineurin 1 (RCAN1)

1.3.1 RCAN1 structure and location.

This study is focused on the metabolic effects of regulator of calcineurin 1 (RCAN1) encoded by a gene located on chromosome 21 in human, people with down syndrome have an extra copy of the same chromosome (Fuentes et al., 2000) (Fig. 1a). They are more likely to get type 2 diabetes. RCAN1 is primarily expressed in white adipose tissue, liver, brain, heart and skeletal muscle, adrenal gland and pancreas. RCAN1 inhibits calcineurin activity in human and mice models (Fuentes et al., 2000)

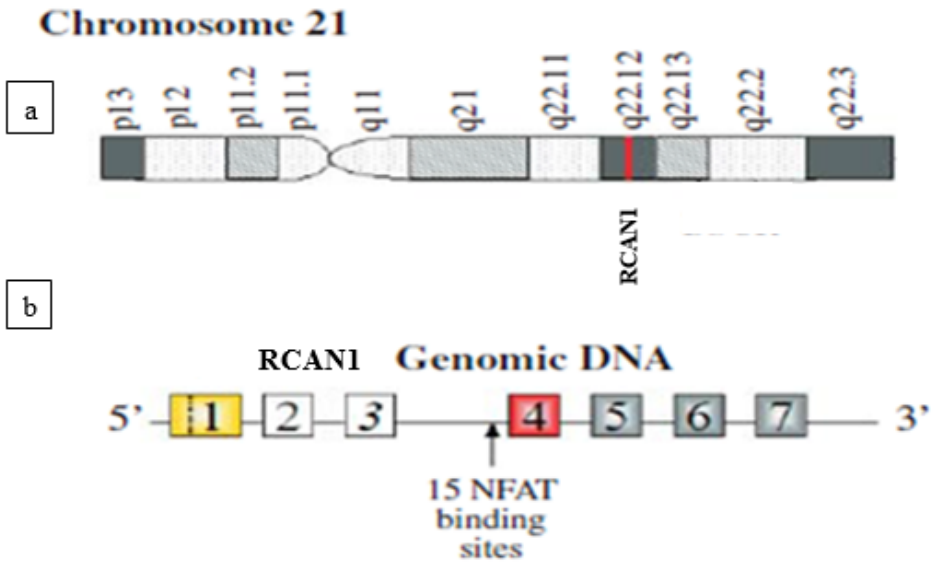

Figure 1.1 RCAN1 Location.

a. Position of RCAN1 on chromosome 21 in region q22.12.

b. RCAN1 is consist of seven exons. RCAN1 has two main isoforms named RCAN1.1 and RCAN1.4.

The *RCAN1* gene in human and mice encodes two main isoforms named RCAN1.1 and RCAN1.4, depending on the exon at which transcription is initiated (Fig. 1b). RCAN1.1 regulates exocytosis, learning, memory, synaptic transmission, β-cell function and insulin secretion, and immune cell function (Keating et al., 2008, Peiris et al., 2012). RCAN1.4 is expressed at lower levels than

RCAN1.1 and is highly up-regulated in response to oxidative stress (Lee et al., 2009). Overexpression of RCAN1.4 causes apoptosis in neurons, however when RCAN1.4 expression is knocked down, cell growth slows down due to inhibition of Ras and apoptosis is protected against (Lee et al., 2009).

2.2 RCAN1 and Calcineurin pathway.

RCAN1 has a well-known role as an endogenous inhibitor of the phosphatase calcineurin (Fig 1.2).

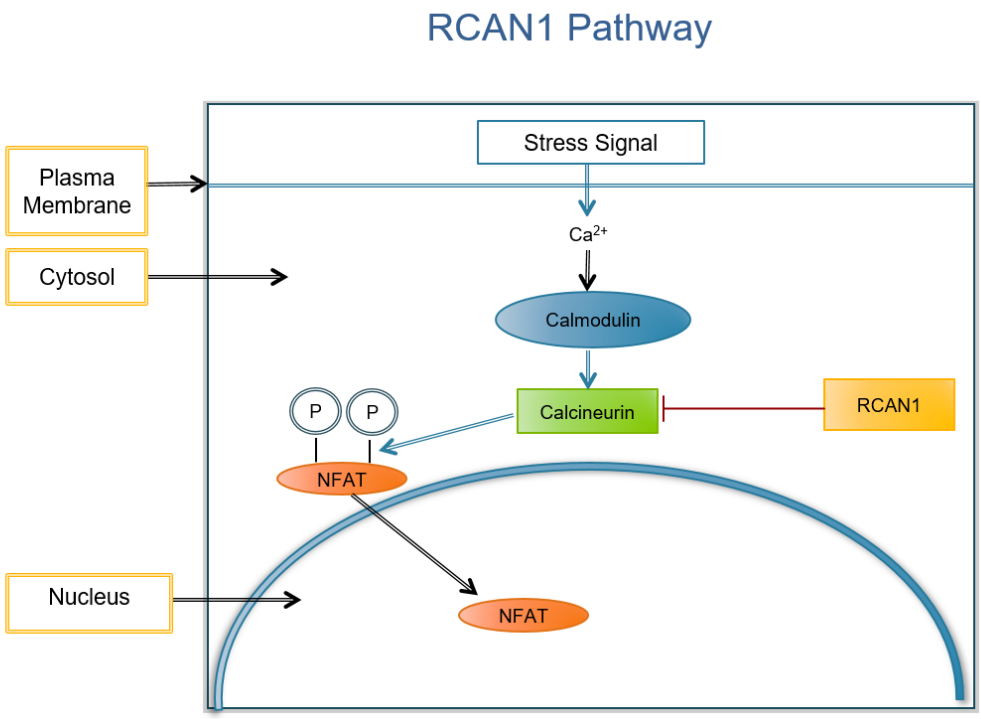

Figure 1.2 RCAN1 And Calcineurin Pathway.

Calcineurin is found in many tissues, including liver, adipose tissue, pancreas, heart, brain, adrenal cells, kidney, lung, placenta, eye, and skeletal muscle (Torac et al., 2014). Calcineurin is a calcium- and Calmodulin dependent serine/ threonine phosphatase, and NFAT is one of its important substrates (nuclear factor of activated T cells). The NFAT protein is a transcription factor first identified in the immune system, and so it is critically important for the immune response (Rao et al., 1997). Dephosphorylation of NFAT by calcineurin activates it, enabling it to enter the nucleus to activate transcription of genes involved in the immune response (Torac et al., 2014). Calmodulin is a calcium dependent calcineurin binding protein, which activates calcineurin, allowing it to

dephosphorylate NFAT. However, when RCAN1 is expressed in the cell, it inhibits calcineurin activity, which can inhibit NFAT transcription factor activities Figure 1.2 (Vega et al., 2003).

.

1.3.2 Role of RCAN1 in obesity.

Fat cells (adipocytes), from adipose tissues are fibrous connective cells responsible for triglyceride storage. These cells have been found to play a crucial role in the development of obesity-related comorbidities like insulin resistance. Unpublished data from our lab shows that RCAN1 knockout mice fed a high fat diet gain very little fat mass compared to wild-type mice on the same high fat diet.

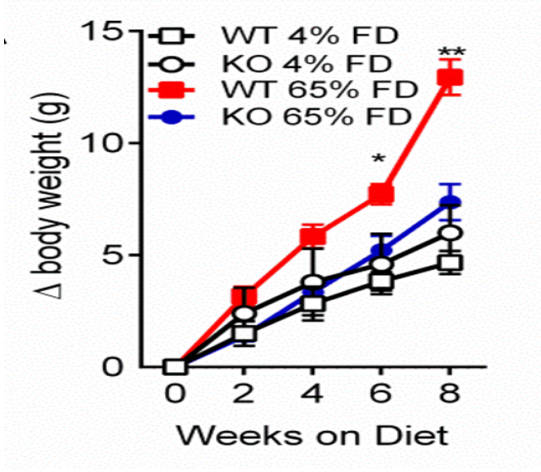

Figure1.3 Rcan1-/- mice are protected from obesity.

Comparison of *Rcan1*$^{-/-}$ mice (KO) vs. wild-type mice (WT) after 8 weeks on a 4% or 65% fat diet (FD).

This data indicates that knockout mice were protected from obesity compared to wild-type mice after being fed a high fat diet for 8 weeks (65% FD). Also it shows that there is no significant difference between knockout and wild-type mice after a low fat diet (4% FD).

In a genetic screen of 108 strains of mice, it was observed that in adipose tissue, RCAN1 expression correlates to different measures of impaired metabolic control (Parks et al., 2015). This is supported by another study on mice by Keller et al. that provides evidence for a correlation between a decrease in metabolism and increased RCAN1 expression in white adipose tissue (Keller et al., 2008). The functional relevance of these findings was examined by our laboratory, the data showed

that *Rcan1*$^{-/-}$ (knockout) mice put on less weight compared to wild-type mice under a high fat diet (unpublished).

Considering the connection between RCAN1 and obesity and the link between obesity and insulin resistance, we were interested in whether the expression of *Rcan1* changes in relation to risk factors of those conditions such as age, high fat diet, in metabolic tissues such as adipose tissue and liver.

1.4 Thermogenesis.

1.4.1 Thermogenesis and Obesity.

Definition of thermogenesis

Thermogenesis is defined as the process of cellular heat production. There is a relationship between thermogenesis and body weight. White adipose tissue contains inducible brown adipocytes called beige adipocytes; these can increase weight loss and whole body thermogenesis in a process called adipocyte 'browning' (Wu et al., 2012). Loss of RCAN1 expression leads to anti-obesity effects due to the increase in fat thermogenesis under high fat diet conditions. Unpublished data from our lab illustrates that *Rcan1*$^{-/-}$ mice show an improvement in the thermogenesis program in response to the inducing stimulus of a high fat diet in subcutaneous white adipose tissue (WAT) (Keating et al. unpublished data).

In this study, we measured the expression of different adipocyte genes associated with fat thermogenesis in *Rcan1*$^{-/-}$ knockout and wild type mice.

1.5 Inhibitors of RCAN1-Calcineurin association.

Five small molecules that inhibit *Rcan1* have been identified by Chan et al. (B. Chan, 2007) (Table 1). Overexpression of RCAN1 is associated with diabetes (Peiris et al., 2012, Peiris et al., 2016). In the absence of *Rcan1*, mice are resistant to diet induced obesity and glucose intolerance. Decreasing the function of RCAN1 would be a good therapy for obesity. We wish to test these drugs on fat cells to see if they can reduce fat mass.

Our unpublished data suggests that obesity and type 2 diabetes (T2D)-associated β-cell dysfunction can be reduced through RCAN1 inhibition. Therefore, our laboratory aims to develop therapeutic leads targeted against RCAN1. In 2007, Chan et al. (B. Chan., 2007) used a fluorescence-based binding assay in a high throughput screen of ~32,000 small molecules in order to identify drugs that interrupt the interaction between RCAN1 and calcineurin. Five lead compounds were identified, which can dose-dependently disrupt RCAN1 binding to calcineurin *in vitro* (Ki values for these 5 small molecules are listed in Table 1.1).

Table 1.1 five inhibitors of RCAN1.

IRCA1-5 and their effective concentrations in μM (B. Chan, 2007).

Inhibition Potencies (Ki values) of IRCAs	
Compound	Ki (μM)
IRCA1	0.99 ± 0.19
IRCA2	2.24 ± 0.26
IRCA3	2.89 ± 0.58
IRCA4	2.49 ± 0.36
IRCA5	1.36 ± 0.20

These compounds function specifically as inhibitors of the RCAN1-calcineurin association (IRCA). Despite inhibiting the RCAN1/calcineurin interaction, these drugs do not inhibit calcineurin activity itself. This is an essential characteristic, since immunosuppressants that target calcineurin, like cyclosporine A, can lead to reversible β-cell dysfunction and diabetes. Since the initial identification of these compounds, no study has been published regarding either the testing of these compounds *in vivo* or their therapeutic application to target RCAN1 function. There are also no patents available regarding possible usage of these compounds in this area. The fact that an anti-obesity phenotype in *Rcan1*$^{-/-}$ mice has not yet been reported has provided us with a unique

opportunity to test the impact of these compounds as possible new therapeutics for treatment of obesity and diabetes.

1.6 The 3T3-L1 adipocyte cell lines.

1.6.1 Origin of 3T3-L1 cells.

The 3T3-L1 cell line is a pre-adipose cell type, which was initially established from murine Swiss 3T3 cells by clonal expansion (Green and Kehinde, 1974, Zebisch et al., 2012). The cell line has been extensively used because of its ability to differentiate from fibroblasts to adipocytes.

1.6.2 Differentiation of 3T3-L1 cell lines into adipocytes.

3T3-L1 cells can be converted from their fibroblastic phenotype to adipocytes; they are usually treated with pro-differentiating factors after the cells undergo growth arrest. The most commonly used agents used to induce differentiation of the 3T3-L1 cells from fibroblasts to adipocytes are insulin, biotin, dexamethasone (Dex), and 3-isobutyl-1-methylxanthine (IBMX). It is known that insulin binding to the insulin receptor activates the pathway signaling that causes the rapid insertion of glucose transporters into the plasma membrane of a fat or muscle cell, greatly increasing glucose intake (Alberts et al.).

It is known that the decrease or increase of fat cell size is regulated directly by hormones, such as insulin or the levels of circulating nutrients, that reflect nutrient levels in adipose tissue (Alberts et al.). Approximately 4 days after adding the differentiation factors, the cells start to create lipid droplets that increase in number and size over time.

Unpublished data from a collaborator of our laboratory, Dr Beverly Rothermel, indicates that when RCAN1 expression is knocked down in 3T3-L1 cells and they are induced to differentiate, they produce less lipid droplets. This is a useful phenotype that can be used to measure and to see how modifying Rcan1 levels effects fat production. Based on this phenotype we use this model to test the function and ability of the drugs.

1.7 Aims and hypotheses:

This study contains three hypotheses. These form the basis of our study on the role of *Rcan1* in metabolism.

1.7.1 Aim and hypothesis 1

Aim 1:

Determine the expression of *Rcan1* in white adipose tissue in relation to age and diet.

Hypothesis 1:

Age and diet will affect the expression of *Rcan1* in adipose tissue.

1.7.2 Aim and hypothesis 2

Aim 2:

Measure the effect of RCAN1 on the expression of adipocyte genes associated with fat thermogenesis.

Hypothesis 2:

Loss of RCAN1 expression has an anti-obesity effect by increasing fat thermogenesis under high fat diet conditions.1.7.3 Aim and hypothesis 3

Aim 3:

Test whether the five IRCA compounds, which inhibit RCAN1, can affect RCAN1-associated *in vitro* metabolic phenotypes.

Hypothesis 3:

Chemical inhibitors of RCAN1 will decrease adipocyte fat content.

The objective of this work is to help determine the role of RCAN1 action in adipocyte biology, by identifying the effects of RCAN1 on fat mass and changes in its expression in relation to age and diet. Furthermore, there will be a focus on the expressions of thermogenesis genes by comparing them in Rcan1$^{-/-}$ and Rcan1$^{+/+}$ white adipose tissue. Finally, we focus on chemical inhibitors of RCAN1 function and whether they can affect adipocyte function.

2. Materials and Methods:

2.1 Extraction of total RNA from white adipose tissue:

White adipose was obtained from Rcan1 null mice (Flinders) or wild-type generated on a mixed 129SvJ × C57BL/6 genetic background. Mice were fed either a normal chow diet (4% calories as fat) or a high fat diet consisting of 35% calories as fat. Total RNA was extracted from white adipose tissues using the RNeasy® Lipid Tissue Mini Kit (Qiagen, Australia) by following the manufacturer's instructions.

1ml of QIAzol Lysis Reagent was added to ≤100mg of white adipose tissue. Then, a stainless steel bead was added to the tube. The tissue was homogenized using Tissuelyser (Qiagen, Australia) for 5 minutes at a frequency of 30 Hz. The sample was incubated at room temperature for 2 minutes and then 200µl of chloroform was added. The sample was mixed by shaking the tube vigorously for 15 seconds, followed by a 3 minutes incubation at room temperature. The sample was then centrifuged at 10000 x g for 15 minutes at 4°C, which separated the sample into 4 phases: 1) an upper or aqueous phase, 2) a white interphase, 3) an organic phase, 4) a clear lower phase (Figure 2.1). The aqueous phase containing the RNA was transferred to a clean RNeasy spin column, which was placed in a 2ml collection tube, and 1 volume of 70% of ethanol was added and the sample was mixed thoroughly by vortexing.

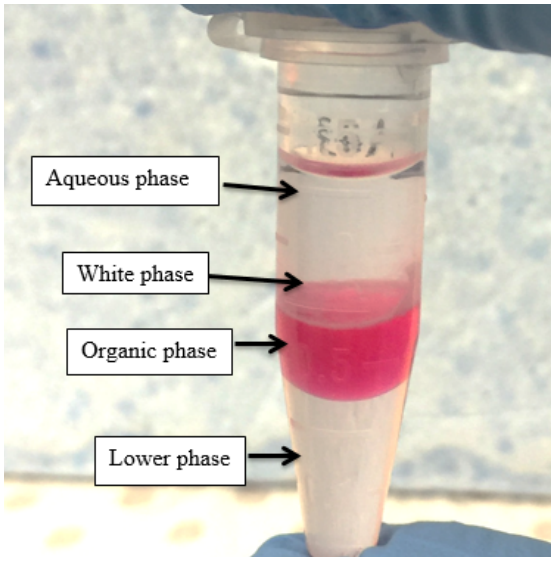

Figure 2.1 RNA Purification from White Adipose Tissue

Four separate phases are distinguishable from white adipose tissue using the RNeasy® Lipid Tissue Mini Kit extraction method. The sample was separated into 4 phases, an upper or aqueous phase containing the RNA, then a white interphase, followed by an organic phase, and a clear lower phase.

A 700µl volume of the sample was transferred to an RNeasy column within a collection tube, centrifuged for 15 seconds at 10000 x g and the flow-through was discarded. The remainder of the sample was added to the same column and centrifuged again. The column membrane was washed with 350µL of buffer RW1 and the flow-through was discarded. Then a mixture of 70µL of RDD buffer and 10µL of DNase I was added directly to the membrane and the sample was incubated at room temperature for 15 minutes. Another 350µL of buffer RW1 was used to wash the column again, with centrifugation at 10000 x g for 15 seconds. Then 500µL of RPE buffer was added to wash the RNeasy column, with centrifugation for 15 seconds at 10000 x g. The flow-through was discarded and then the previous wash step was repeated using a fresh 500µL volume of RPE buffer, with centrifugation for 2 minutes. For RNA elution, the RNeasy column was placed in a fresh 1.5 mL tube; 30µL of RNase-free water was added directly to the membrane and centrifuged through the column for 1 minute at 10000 x g. To increase yield, the eluted RNA solution from the previous step was added to the same RNeasy column and centrifuged through the column again. The concentration of the purified RNA was measured using a NanoDrop 2000™ (Thermo Scientific, Australia) and stored at -80°C until it was required. The quality of the RNA was assessed prior to cDNA synthesis using a 2100 Bioanalyzer Instrument (Agilent).

2.2 Reverse-transcription cDNA synthesis using Oligo dT:

The cDNA synthesis was performed using the Omniscript® RT Kit (Qiagen) by following the manufacturer's instructions. For each reverse transcription reaction, 200ng of RNA was used. The

reverse transcription reaction mix was prepared as in Table 2.1 below. After adding the required components, the tube was incubated in a 37°C water bath for an hour.

Table 2.1 Reverse transcription reaction components.

Component	**Volume per reaction**
Template RNA (200ng)	*x*µL
RNase-free water	(12-*x*) µL
10 x Buffer RT	2µL
dNTP Mix (5mM each dNTP)	2µL
Oligo-dT primer (10µM) (Qiagen)	2µL
RNase inhibitor (Ambion) (10 units/µl)	1µL
Omniscript® Reverse Transcriptase (Qiagen)	1µL
Total Volume	20µL

2.3 Quantitative Real-Time PCR using SYBR® Green:

Quantitative real-time PCR was performed using the Qiagen Quantitect® SYBR® Green PCR kit and Rotor-Gene 3000 thermocycler (Corbett Research). The 18s ribosomal RNA gene was used as the housekeeping gene to normalize the reaction, since it is highly expressed, very abundant and expressed in all cell types. Master Mix of each quantitative real-time PCR reaction was freshly prepared as in Table 2.3. The total volume of each reaction after addition of cDNA was 25µL. All samples were run in triplicate. All quantitative PCR (qPCR) runs had a negative control, in which 2µL water was added instead of cDNA.

Table 2.2: List of genes that were used in our real time PCR experiments.

The table illustrates the common names of the genes with their forward and reverse sequences.

Table 2.2 List of genes that were used in our real time PCR experiments.

Gene	Forward	Reverse
18s ribosomal RNA	CCCTGCCCTTTGTACACACC	CGATCCGAGGGCCTCACTA
Rcan1	CAAGGACACCACCTTCCAGT	GGAACTGTTTGTCGGGATTG
Rcan1.1	ATGGAGGAGGTGGATCTGC	TTTATCCGGACACGTTTGAAG
Rcan1.4	CTGATTGCTTGTGTGGCAAA	GCAGATAAGGGGTTGCTGAA
uncoupling protein 1 (*Ucp1*)	GCCAAAGTCCGCCTTCAGAT	TGATTTGCCTCTGAATGCCC
Pparγ coactivator 1 alpha (*Pgc1α*)	CCCAGGCAGTAGATCCTCTTCAA	CCTTTCGTGCTCATAGGCTTCATA
peroxisome proliferator-activated gamma (*Pparγ2*)	GCATCAGGCTTCCACTATGGA	AAGGCACTTCTGAAACCGACA
carnitine palmitoyltransferase I (*Cpt1a*)	GTGACGTTGGACGAATCGGA	TCGGTGGCCATGACATACTC
Monocyte chemoattractant protein-1 (*Mcp-1*)	GGCTCAGCCAGATGCAGTTAAC	GCCTACTCATTGGGATCATCTTG
Tumor necrosis factor-alpha (*Tnf-α*)	GTACCTTGTCTACTCCCAGGTTCTCT	GTGTGGGTGAGGAGCACGTA

Table 2.3 Quantitative real-time PCR reaction components prior to addition of cDNA.

Components	Volume/reaction
SYBR® Green qPCR master mix (2X)	12.5µL
Forward Primer (10µM)	0.75µL
Reverse Primer (10µM)	0.75µL
Nuclease-free water	9µL
Total Volume	23µL

The reaction mix totalling 23µL/reaction was aliquoted into 0.1mL Axygen PCR Tubes, followed by the addition of cDNA (2µL/reaction) to appropriate sample tubes. The samples were run using the thermocycler conditions described in **Error! Reference source not found.**2.4.

Table 2.4: Reaction Cycling Conditions of the Rotor-Gene 3000 thermocycler.

PCR Cycle	Condition
Hold	95°C (15 minutes)
Annealing	55°C (20 seconds)
Extension	72°C (25 seconds)
Denaturation	94°C (15 seconds)
Hold	72°C (4 minutes)
Hold	60°C (15 seconds)
Melt	60°C to 99°C

2.4 Agarose gel electrophoresis:

A 3% agarose gel was prepared by mixing 4.5 grams of multi-purpose agarose gel powder in 150mL of 1x TBE buffer. The agarose mix was dissolved by heating using a microwave for 2 minutes. The agarose gel solution was then cooled down to ~ 60°C, following by mixing in 7.5µL of Gel Red™ (Sigma) to detect amplified DNA. With two combs in place, the gel solution was

poured into the tray and left to solidify for 35 minutes at room temperature. The combs were then removed from the gel and the gel placed in the buffer chamber and covered with 1x TBE buffer. 2µL of 6x Loading Dye (Sigma) was mixed with 10µL of the sample. The DNA ladder (1Kb Plus, Invitrogen) was prepared at a concentration of 200 ng/µL. 5µL of the prepared ladder was mixed with 2µL of the 6x Loading Dye (Sigma). After loading the samples, the gel was run at 80V for 45 minutes. The gel was imaged using Image Lab™ Software (Bio-Rad) under ultra-violet light utilising the Gel Doc EZ Imager (Bio-Rad) at an exposure time of 0.5 seconds.

2.5 3T3-L1 cell line:

2.5.1 Preparing media for 3T3-L1 cells.

Table 2.5: Maintenance medium components.

Component	Volume	Supplier
DMEM (high glucose 4.5g/L)	500mL	Thermo Fisher Scientific, Australia
Fetal Bovine Serum, mesenchymal stem cell-qualified (FBS-MSC)	50mL	Thermo Fisher Scientific, USA
Penicillin, 10^5 Units/mL: Streptomycin, 10^5 µg/mL (100x Pen/Strep)	5mL	Thermo Fisher Scientific, Australia

Mesenchymal stem cell-qualified Fetal Bovine Serum (FBS-MSC) was stored at -80ºC. Prior to heat inactivation, a 500mL bottle of FBS-MSC was thawed at room temperature and aliquoted into 50mL aliquots. These aliquots were heat-inactivated by incubating in a 65ºC water bath for 30 minutes. The prepared aliquots were stored at -20 ºC until they were required.

The media was prepared using 500mL of DMEM (high glucose 4.5g/L) (Thermo Fisher Scientific) which was stored at 4ºC. Lastly, 50mL heat- inactivated FBS-MSC and 5mL of *Penicillin* (10^5 Units/mL)/*Streptomycin* (10^5µg/mL) were added to 445mL of the DMEM.

2.5.2 Seeding 3T3-L1 cell line from frozen stock:

3T3-L1 cells (passage number 12) were obtained from Prof David James (Charles Perkins Centre, Sydney) and stored in liquid nitrogen. The 1.8mL vial that contained 1.5mL of cells (passage #12) was thawed by transferring the tube from liquid nitrogen storage to ice. Then the cells were transferred into a 15mL tube, followed by the addition of 1.5 mL of warmed medium (containing heat- inactivated FBS-MCS). After incubating at room temperature for 5 minutes, the volume was topped up to 10mL. The cells were then spun down at 560 x g for 5 minutes and the supernatant was discarded. 1mL of medium was added to the cells and the tube flicked gently to resuspend the cells. The resuspended cells were transferred to a T25 flask and incubated at 37ºC and 5% CO_2 (SANYO CO_2 incubator). The cells were assessed for viability the following day. The media was changed every second day by taking out 2/3 of the media from the flask and replacing it with the same volume of fresh media.

2.5.3 Splitting the 3T3-L1 cell line.

The cells were usually split three times per week. When the cells became 60% confluent they were split into 6-well plates to prepare them for experiments. The cells were washed with PBS to remove all of the excess media. Trypsin 0.05%/ EDTA 0.02% in calcium and magnesium-free saline (CMFS) was added and the flask incubated for 3 minutes to allow the trypsin/EDTA to dislodge all of the cells from the flask. DMEM was added to the cells to stop the reaction by trypsin and cells were transferred into a 15 mL tube and centrifuged at 560 x g for 5 minutes. The supernatant was discarded and 13 ml of media was added. The cells were resuspended by thorough mixing and 0.5 ml of the cells transferred to each well. In addition, 1 mL of the cells was transferred into a T125

flask, which contains 9mL of media to keep the cells growing. Finally, the 6 well plates and the growing. The cells were incubated at 37ºC and 5% CO_2.

2.5.4 Differentiating 3T3-L1 cells to adipocytes.

When the cells were 100% confluent (Figure 2.2), they were left for two days to help the cells transition from a growth phase into a differentiation mode. Then the differentiation media was freshly prepared by using media containing 10% of heat- inactivated FBS-MSC and *Penicillin-Streptomycin* along with additional components listed in Table 2.6 below.

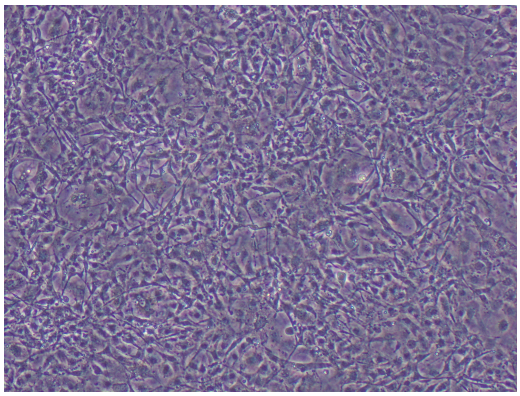

Figure 2.2 100% Confluence of 3T3-L1 Cell line.

The image illustrates plated 3T3-L1 cell line when they are 100% confluent.

Table 2.6: The components of the differentiation media.

Component	**In 50ml of media**
Dexamethasone: 10,000x stock (Sigma – D4902, Mr 392.45) 2.2mM.	5µL
Biotin: 1000x stock (Sigma B4639) 100µg/mL.	50µL
Insulin: 100x stock (bovine, Calbiochem).	25µL
Isobutyl-1-methyl-xanthine (IBMX): 1000x stock (Sigma – I5879, Mr 222.3) 500mM.	50µL

After allowing the cells to differentiate for three days, all of the media was removed from the wells and replaced with post-differentiation media and then incubated for three days at 37ºC/ 5% CO_2. The post-differentiation media was freshly prepared by adding the components in Table 2.7

Table 2.7: The components of the post-differentiation media.

Component	**Volume**
DMEM (high glucose 4.5g/L)+ 10% (FBS-MSC) and 0.5% Pen-Strep	50 mL
Insulin: 100x stock (bovine, calbiochem).	25 µL

2.5.6 Maintaining adipocyte cells.

After post-differentiation, the cells were switched to normal media (DMEM + 10% FCS-MSC, and Pen/Strep). The media was refreshed by removing 2/3 of it and replacing it with the same volume of new media every second day. Differentiation of 3T3-L1 cells into adipocytes takes approximately three weeks from the data of first plating.

2.5.7 Oil Red-O staining for adipocytes.

Cells were washed with phosphate-buffered saline (PBS) twice for 10 minutes. The PBS was removed and then 4mL of 10% formalin was added to each well followed by incubation at room temperature for an hour to fix the cells. After fixing, the cells were washed with 60% isopropanol for 10 minutes to equilibrate the cells prior to Oil Red-O staining. Oil Red-O stain is solvent in 0.5% isopropanol (Sigma) was diluted in 60% of isopropanol, the final concentration of Oil Red O was 60%. Then, 4mL of the prepared stain was added to each well and incubated for 20 minutes at room temperature. The cells were then washed with water five times. The cells were then visualised

under a light microscope and images were taken to make sure that Oil Red-O dye stained all of the fat droplets (OLYMPUS CKX41 microscope). Oil Red-O stain was eluted from the cells by incubating them with 800µL of 100% isopropanol at room temperature for 10 minutes. Then 1mL of 60% isopropanol was added to increase the volume of the solution. The solution was mixed several times by pipetting up and down to make sure that all Oil Red-O was eluted. Subsequently, 250µL of each sample was transferred to individual wells of a 96-well plate. The Oil Red-O absorbance (at 560nm) was read using a plate reader (BECKMAN COULTER® -DTX 880 Multimode Detector). Multimode software was used to visualize the results. Then results were compared using GraphPad Prism.

The negative control wells contained 60% isopropanol (used as blanks). The Oil Red-O stain standard was prepared as in Table 2.8 below.

Table 2.8: Oil Red-O Standard preparation:

The table shows the concentrations of oil red-O standard using 60% of oil red-O and 60% of isopropanol in (µL) (Whitehead et al., 2004).

	Oil Red-O Working solution (µL)	60% isopropanol (µL)
Blank	0	1000
1/64 dilution	16	984
1/32 dilution	31	969
1/16 dilution	63	938
1/8 dilution	125	875
1/4 dilution	250	750

2.5.8 Adipocyte viability test:

The viability test was done using Trypan Blue staining. The cells that were plated in wells of a 6-well plate were first washed with PBS to remove the medium. Then, 1 mL of PBS and 1mL of 4% Trypan Blue were placed in each well. The cells were incubated for 2 minutes at room temperature and then the trypan blue solution was removed and the cells were washed 3 times with water to remove all of the excess stain. The cells were visualised under a microscope for a viability check. The cytoplasm is clear in appearance in viable cells, whereas the cytoplasm is blue in nonviable cells (Strober, 2001).

2.6 Effect of IRCA drugs on the 3T3-L1 cell line.

Table 2.9: Inhibitors of RCAN1-Calcineurin Association.

The table illustrates five different compounds that inhibit RCAN1. It shows also the effective concentration of each drug. All drugs were dissolved in DMSO.

Compound	Concentration (µM)	Supplier
IRCA1 (Norfluoxetine)	0.99 x 1000µM	Sigma-Aldrich
IRCA2	2.24 x 1000µM	Ambinter, France
IRCA3 (Sulconazole nitrate)	2.89 x 1000µM	Sigma-Aldrich
IRCA4 (Heterocyclic carbonyl)	2.49 x 1000µM	Ambinter, France
IRCA5	1.36 x 1000µM	Ambinter, France

2.6.1 Effect of IRCA drugs on the differentiation of the 3T3-L1 cell line:

When the cells were 100% confluent in a 6 well-plate, they were left for two days to prepare them for differentiation. Then 4µL of each of the IRCA drugs (Concentration is shown in Table 2.9) was diluted in 4mL of the differentiation media and added to the cells. One of the wells was used as a negative control (differentiation media only). The media was changed every day by removing all of the media from the wells and replacing it with fresh media that contained the drugs prepared starting from initial differentiation date. The total treatment period was for 12 days. The effect of the drugs was measured using Oil Red O absorbance.

2.6.2 The effect of IRCA drugs on post-differentiation of the 3T3-L1 cell line:

When the cells were 100% confluent, they were left for 2 days in the incubator at 37°C. Then the differentiation media was added to the cells, and incubated at 37°C for three days. After three days of differentiation ~ 95- 100% of the cells contained fat droplets. At this stage, IRCA drugs were diluted in post-differentiation medium by mixing 4µL of each drug (concentration of each drug shown in Table 2.9) with 4mL of the media. After 3 days of post-differentiation, the media was switched to normal media containing the IRCA drugs and cells were incubated for a further 6 days. The media and the drugs were replaced every day from the first date of post-differentiation. The drug treatment was for a total 9 days.

2.6.3 The effect of IRCA drugs on differentiated 3T3-L1 cells.

When the 3T3-L1 cells were 100% confluent, they were left incubating for two additional days. Differentiation media was added to the cells, and they were incubated at 37°C for three days. Then post differentiation media was then added to the cells, which then incubated for 3 days. At this point, post-differentiation and the cells were incubated for three days, which caused the cells to contain bigger lipid droplets. The media was then switched to normal media with the addition of

4μL of IRCA drug (concentration as shown in Table 2.9) per 4mL of media. The media and the drugs were refreshed every day from day 6 until day 12, so the treatment was for 6 days. On day 12 the cells were fixed and stained with Oil Red-O. The absorbance of Oil Red-O was measured using a plate reader as in the previous experiments.

3. Results:

3.1 Expression of *Rcan1* and its isoforms:

3.1.1 *Rcan1* expression in relation to age in white adipose tissue of wild type mice.

Age is considered to be one of the risk factors of obesity. We are focusing on *Rcan1,* which is one of the genes that regulate obesity. As mentioned earlier, there are two main different transcripts of *Rcan1*, which are *Rcan1.1* and *Rcan1.4*. We want to see whether there are any age-dependent expression differepnces of these genes in white adipose tissue in wild type mice. The expression of *Rcan1* measures both transcripts *Rcan1.1*, and *Rcan1.4* in white adipose tissue. All expression levels were measured by real-time PCR. The expression was normalised to 18s ribosomal RNA. As shown in Figure 3.1, there is no statistically significant difference in the expression of *Rcan1* or either of its isoforms.

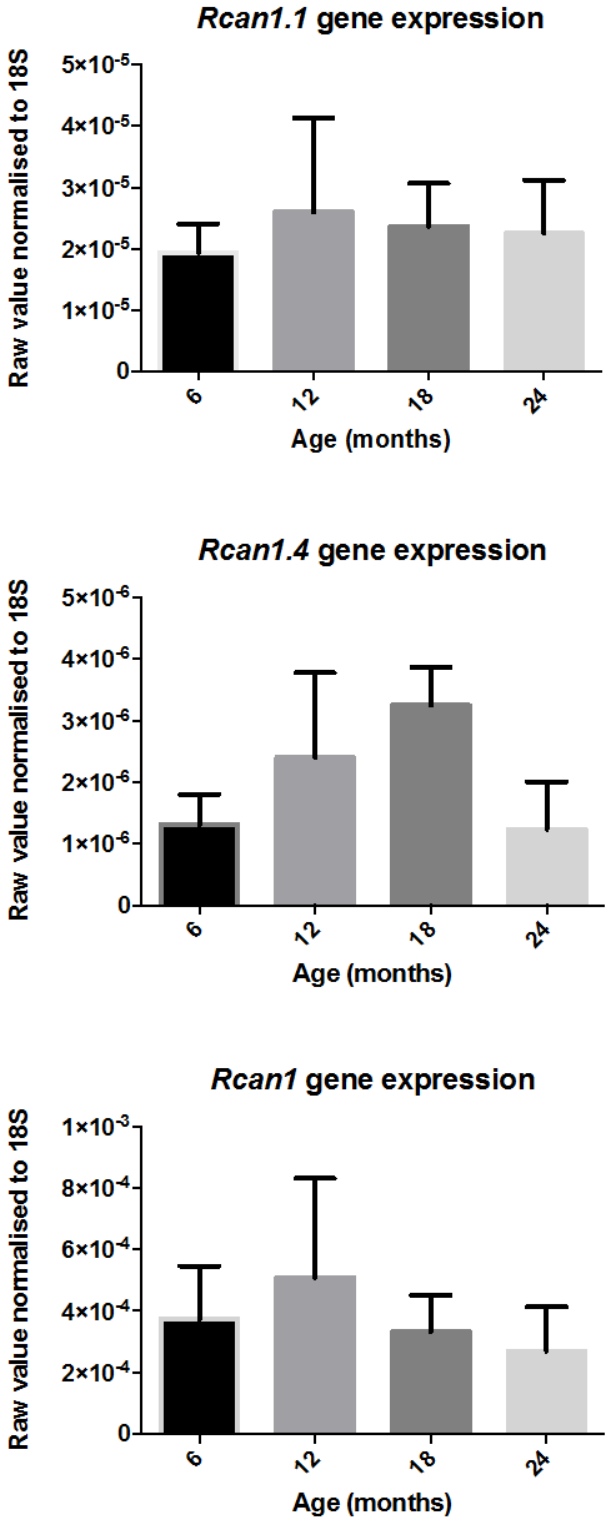

Figure 3. 1 The expression of *Rcan1.1*, *Rcan1.4*, and *Rcan1* over different ages

The expression of *Rcan1.1*, *Rcan1.4*, and *Rcan1* over different ages (6 months, 12 months, 18 months and 24 months) in white adipose tissue from wild-type mice. Statistical analysis was done using GraphPad Prism 6; n=4 except one excluded outlier value from 18 months sample in *Rcan1.1* and *Rcan1* expressions. Values shown are mean ± SEM. This data has been normalised to the 18s ribosomal RNA (housekeeping gene). Quantitative real time PCR was used to compare transcript

levels of *Rcan1.1*, *Rcan1.4* and *Rcan1* genes. Statistical significance was determined using One way ANOVA; $p < 0.427$.

3.1.2 *Rcan1* expression in relation to diet in wild type mice in white adipose tissue.

At 10 weeks old, wild-type mice were put on either a low fat diet or a high fat diet (35%) for 8 weeks and then white adipose tissue was extracted and RNA was purified. The expression of *Rcan1*, *Rcan1.1*, and *Rcan1.4* was measured by real-time PCR and normalised to 18s ribosomal RNA. The expression of *Rcan1*, *Rcan1.1*, and *Rcan1.4* were higher in white adipose tissue from mice fed a high fat diet compared to a low fat diet. However, the difference was not statistically significant.

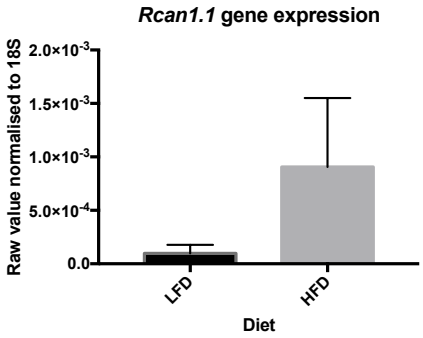

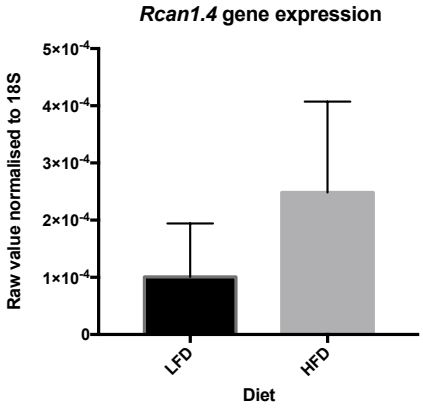

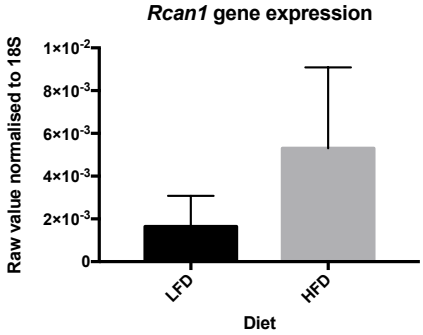

The expression of *Rcan1*, *Rcan1.1*, and *Rcan1.4* in white adipose tissue after high fat diet in comparison to low fat diet. Quantitative real-time PCR was used to quantify changes in the transcription level of the target genes. The samples were run using Rotor-Gene 6000 (n=3). Statistical analysis was done using GraphPad Prism 6; n=4 for the low fat diet samples and 3 for the high fat diet samples. Values shown are mean ± SEM. The data was normalised to 18s ribosomal RNA and analysed using GraphPad Prism 6 software. Statistical significance was assessed using T-tests, however no changes between the 2 diet groups reached significance.

3.2 Thermogenesis gene expression in white adipose tissue in absence or presence of *Rcan1*.

3.2.1 Comparison between 6 thermogenesis genes in white adipose tissue from wild-type and *Rcan1*$^{-/-}$ knockout mice after a high fat diet.

There is evidence that *Rcan1*$^{-/-}$ mice have higher thermogenesis than wild-type mice after a high fat diet (unpublished data from our lab). Therefore, we decided to study the expression of thermogenesis genes in wild type and *Rcan1*$^{-/-}$ mice in white adipose tissue after a high fat diet.

The expression of a panel of thermogenesis genes, *Ucp1*, *Pgc1α*, *Pparγ2*, *Tnf-α*, *Mcp1*, and *Cpt1-α,* were measured using real time PCR. 18s ribosomal RNA was used as a housekeeping gene to normalise the gene expression. The mean expression of all of the thermogenesis genes, except *Cpt1-α,* was lower in *Rcan1*$^{-/-}$ knockout white adipose tissue compared to wild type after a high fat diet; yet none of the differences in expression were statistically significant Figure 3.3.

Based on other data, it was unexpected to see decreased expression of most of the tested thermogenesis genes in *Rcan1*$^{-/-}$ compared to wild type white adipose tissue. This outcome will be discussed further later.

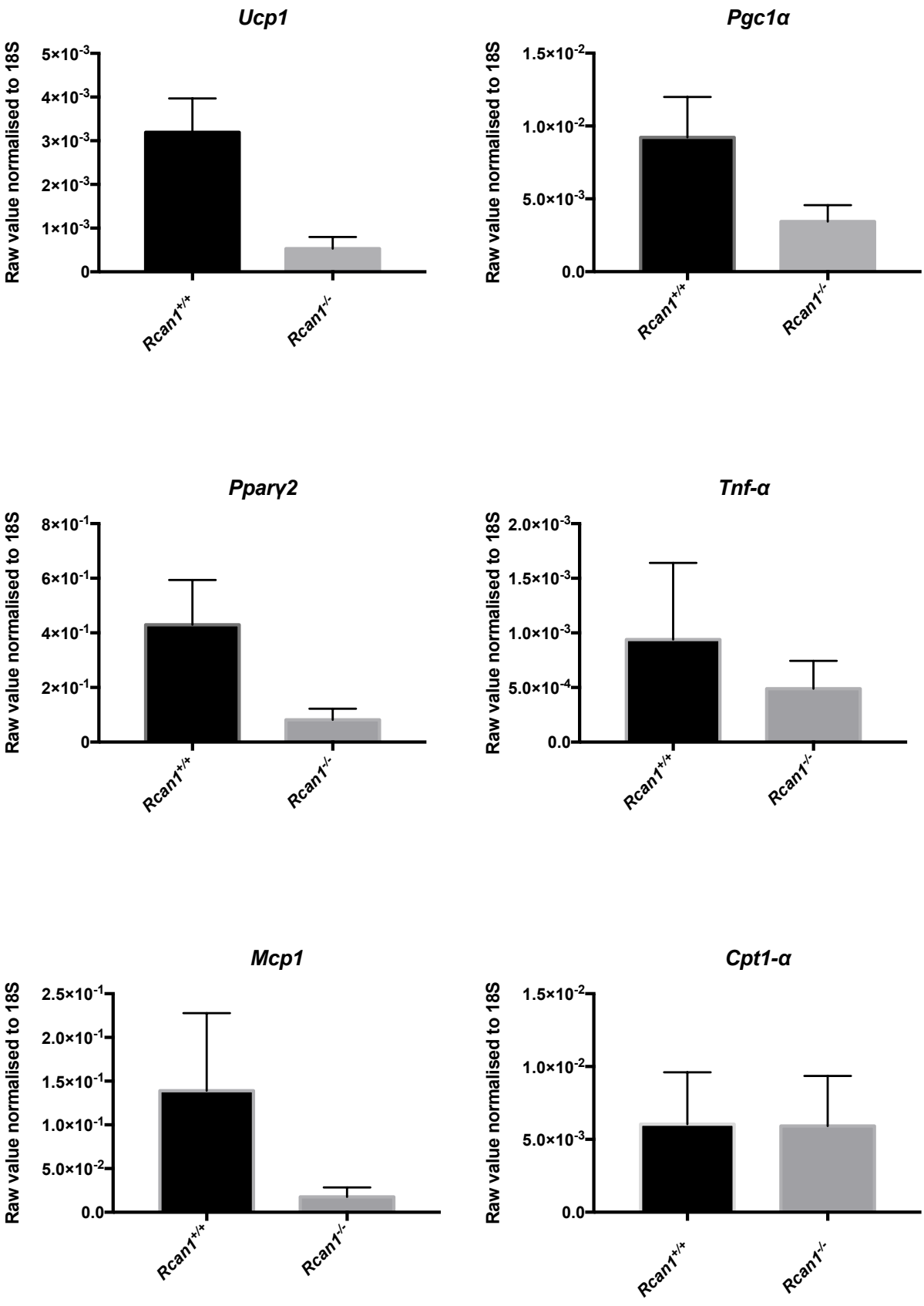

Figure 3.3 Expression of 6 genes associated with thermogenesis in the absence or presence of RCAN1 in WAT after HFD.

The expression of 6 thermogenesis genes in the absence or presence of RCAN1 in white adipose tissue after a high fat diet using quantitative real-time PCR. The data was analysed using GraphPad Prism 6 software, n=3 except for *Ucp1*, there is one excluded value from *Rcan1*$^{-/-}$. This data has been normalised to 18s ribosomal RNA. Statistical significance was determined using T-test; The P values for each gene expression *Ucp1* p= 0.079, *Pgc1α* =0.126, *Pparγ2* =0.108, *Tnf-α* p =0.578, *Mcp1* =0.245, and *Cpt1-α =0.979.*

3.3 Effects of IRCA drug treatments on the 3T3-L1 cell line.

Table 3.1 Experimental timeline for IRCA drug treatment of the 3T3-L1 cell line.

cell line.

	Initial growth of 3T3-L1 cell line	2 days after 100% confluent	Differentiation to adipocytes For 3 days	Post differentiation For 3 days	Maintenance with normal media for 6 days
First Experiment			Drugs added →		
Second Experiment				Drugs added →	
Third Experiment					Drugs added →

3.3.1 The effects of IRCA drugs on 3T3-L1 cell line differentiation:

To see whether these drugs inhibit 3T3-L1 to differentiate to fat cells or not, the drugs were added at the beginning of the differentiation phase. The drug treatment continued throughout the post-differentiation and maintenance phases for a total of 12 days. The cells were fixed with formalin and stained with Oil Red-O. The cells were visualised under a microscope (magnification x10) for red staining (Figure 3.4). These drugs reduced lipid content by different amounts (Figure 3.5). The effect of the drug IRCA2 was significantly higher (smaller fat droplets) compared to the other drugs (Figure 3.4 and Figure 3.5).

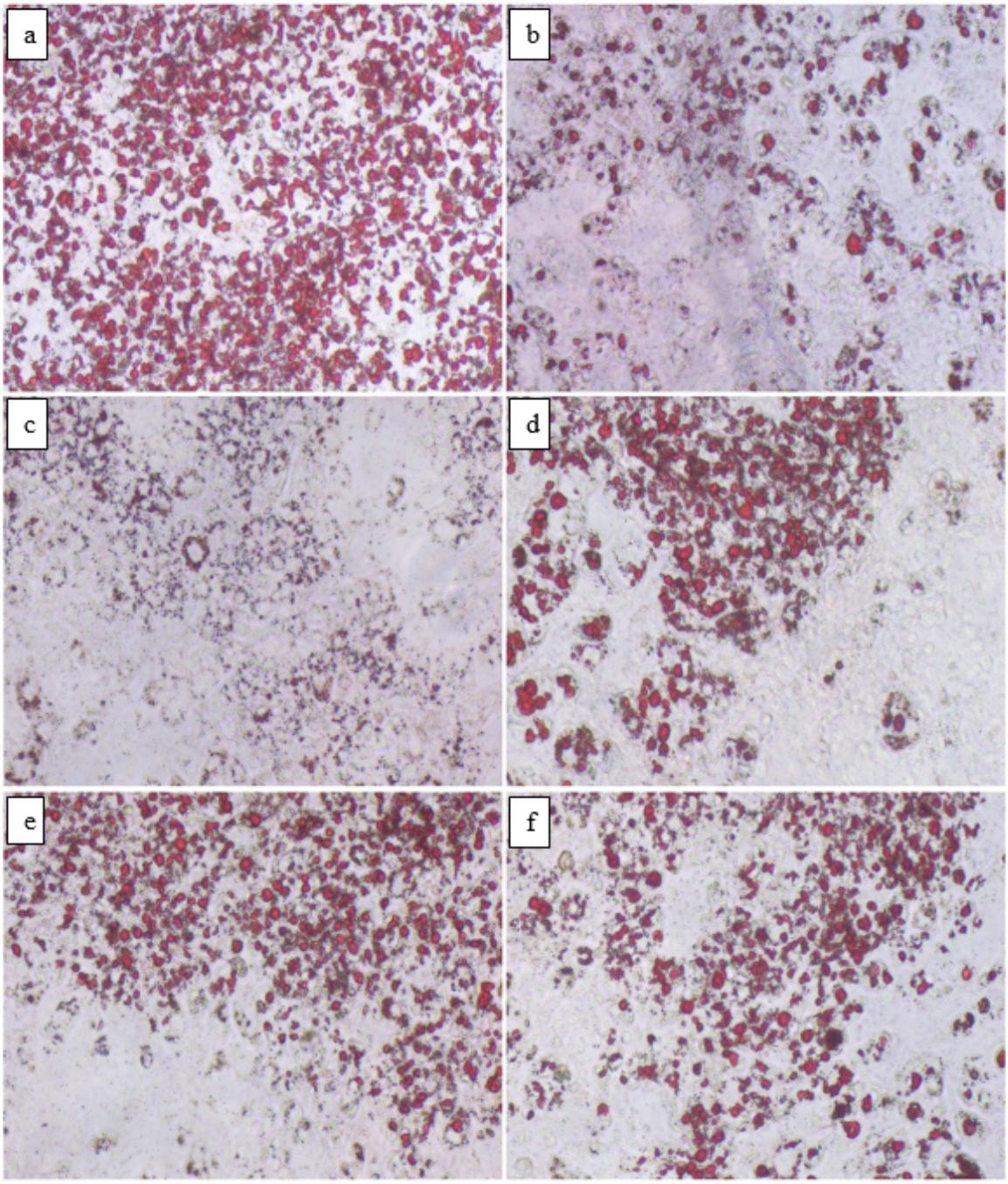

Figure 3.4 Effect of IRCA drugs on the differentiation phase of 3T3-L1 cells

The cells were treated with IRCA drugs for 12 days, starting from the beginning of the differentiation phase, and continued throughout the post-differentiation and maintenance phases. The cells were fixed with formalin, stained with 60% Oil Red-O stain; n=6. Then images were taken using a microscope (magnification x10). Treatments: (a) control (no drugs added), (b) IRCA1, (c) IRCA2, (d) IRCA3, (e) IRCA4, and (f) IRCA5.

Quantitation of Oil Red-O staining in after treating 3T3-L1 cells with IRCA drugs starting from the differentiation phase.

Oil Red-O absorbance was quantitated after treating 3T3-L1 cells starting from the differentiation stage with different IRCA drugs. After fixing the cells, Oil Red-O was applied to stain lipid droplets. The absorbance of Oil Red-O was measured using a plate reader at a wavelength of 560nm. The drugs reduced lipid content compared to the control by the following percentages: IRCA1 (29.6%), IRCA2 (58%), IRCA3 (23.6%), IRCA4 (18.2%), IRCA5 (25.2%). All of the drugs were effective to a different extent, although IRCA4 was not statistically significant. IRCA2 was more than twice as effective as the other drugs, reducing fat content by 58%.

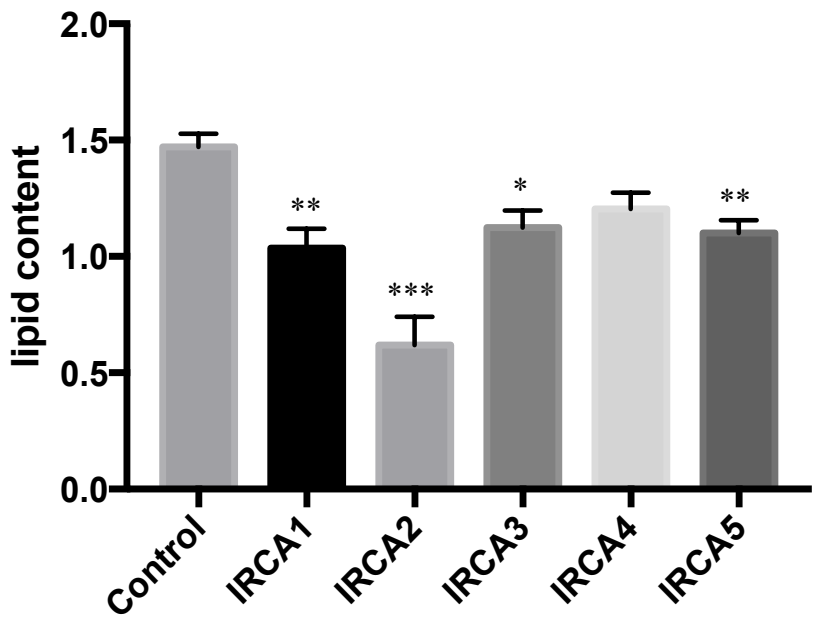

Figure 3.5 Effect of IRCA drugs on the differentiation of 3T3-L1 cells

The cells were treated for 12 days and then fixed and stained with Oil Red-O. The absorbance of the stain was measured using a plate reader at a wavelength of 560nm. Mean absorbance values ± SEM (error bars) are shown. Statistical significance was determined using One way ANOVA; $P<0.0001$. The stars represent the P value (ns $P > 0.05$), (* $P \leq 0.05$), (**$P \leq 0.01$), (*** $P \leq 0.001$), (****$P \leq 0.0001$).

Cells viability after treating them with IRCA drugs starting from the differentiation phase.

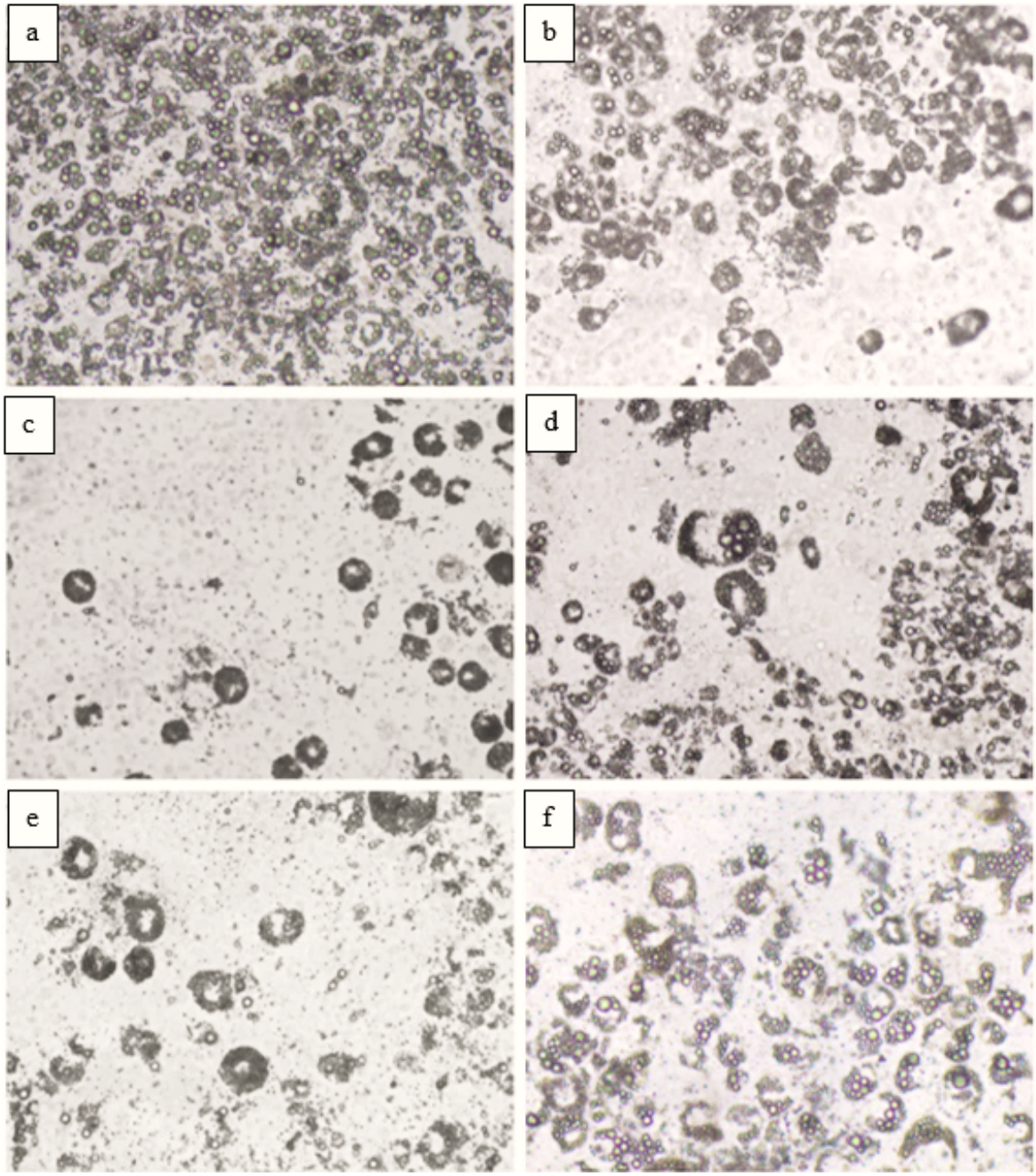

Figure 3. 6 The viability test.

The cells were stained with Trypan Blue staining, then they were visualised under a light microscope. The image illustrates that all of the cells are alive, because clear cytoplasm present viable cells, whereas blue the cytoplasm present nonviable cells. Treatments: (a) control (no drugs added), (b) IRCA1, (c) IRCA2, (d) IRCA3, (e) IRCA4, and (f) IRCA5.

3.3.2 Effect of IRCA drugs on post differentiation of the 3T3-L1 cell line:

The drugs were added on post differentiation, to see whether they can inhibit the cells from growing more fat droplet or reducing them. After differentiation of the cells for 3 days by the addition of

growth factors to convert them into adipocytes (see Methods), all of the cells contained small fat droplets. The cells were then treated with IRCA drugs simultaneously with post-differentiation factors for 3 days and then, 6 days in the maintenance stage. The cells were stained with Oil Red-O. All of the IRCA drugs tested had a significant effect on fat droplet size (Figure 3.7). The effect of IRCA2 was higher compared to the other drugs (Figure 3.7 and Figure 3.8)

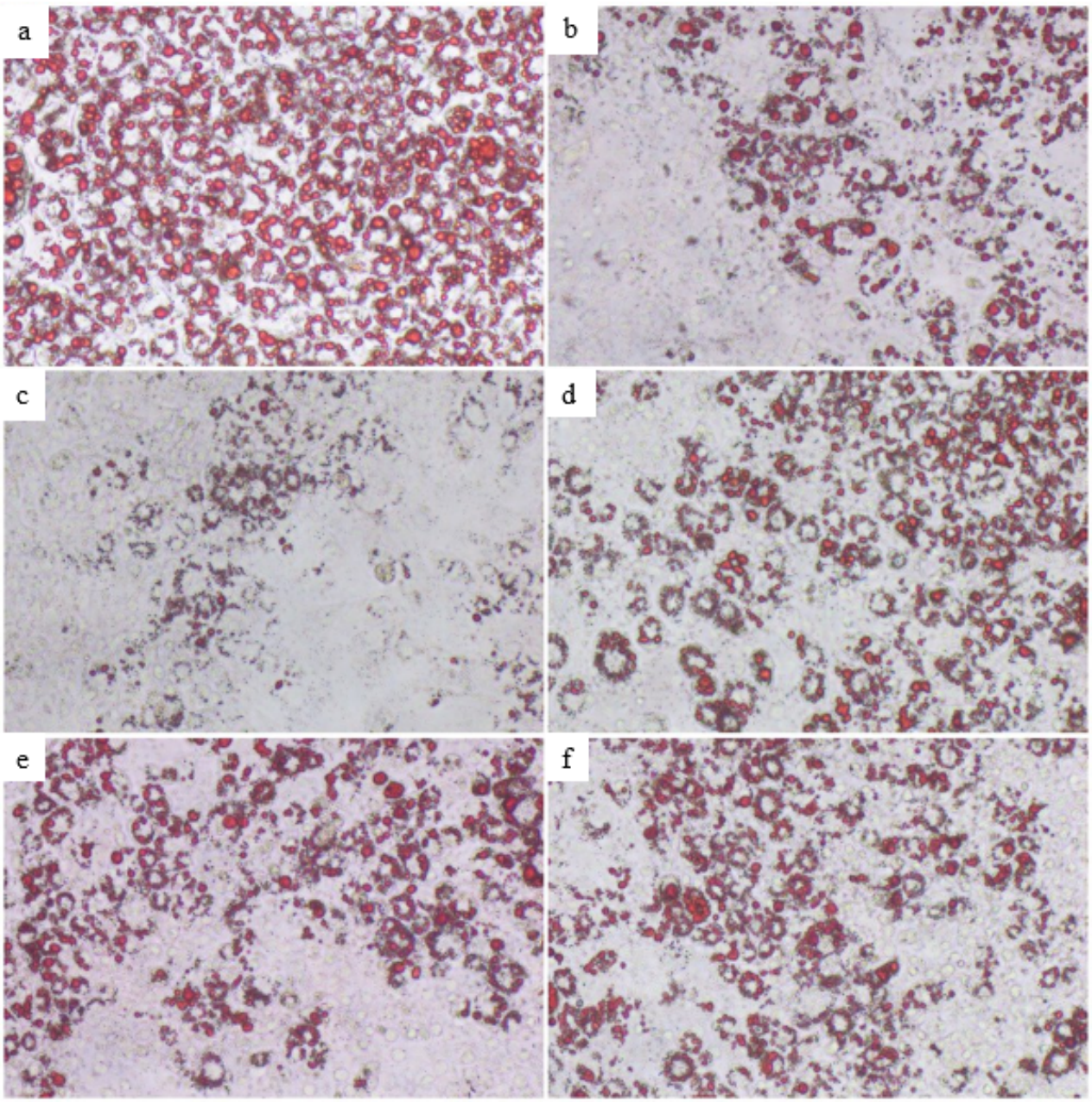

Figure 3.7 Effect of IRCA drugs on post differentiation of 3T3-L1 cells.

Cells were examined after 9 days of treatment. The cells were fixed with formalin, stained with Oil Red-O stain; n=6. These representative images were captured using a light microscope

(magnification x10). (a) is showing the control (no drugs added), (b) IRCA1was added to the cells, (c) IRCA2 which was the most effective drug, the fat droplets in IRCA2 are smaller compared to the control and other drugs, (d) IRCA3, (e) IRCA4, (f) IRCA5.

Oil Red-O quantitation after treating 3T3-L1 cells with IRCA drugs starting from the post-differentiation phase.

After fixing the cells, Oil Red-O was applied to stain lipid droplets. The absorbance of Oil Red-O was measured using a plate reader at a wavelength of 560nm. IRCA drugs had a significant effect in reducing lipid content on 3T3-L1 cell lines after 9 days of treatment. These drugs reduced lipid content by the following percentages: IRCA1 (16%), IRCA2 (54%), IRCA3 (20%), IRCA4 (23%), and IRCA5 (23%).

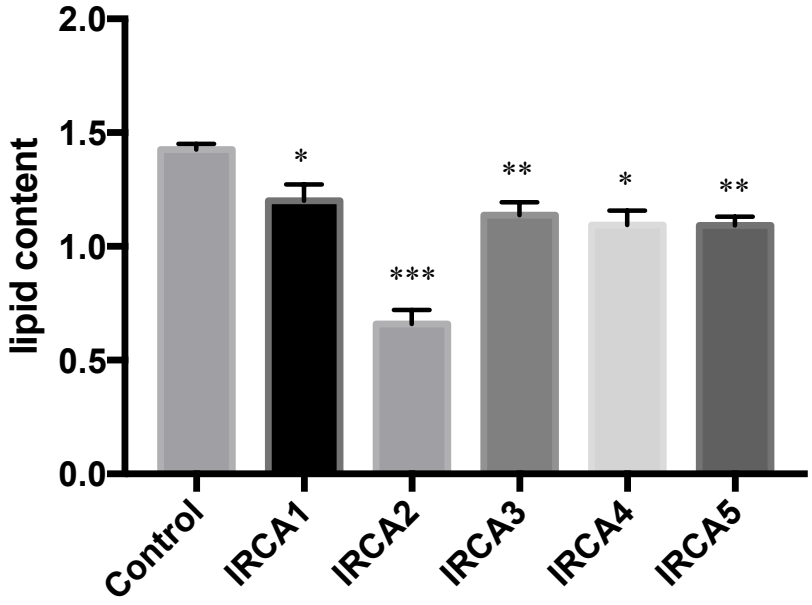

Figure 3. 8 Effect of IRCA drugs on post differentiation of 3T3-L1 cells.

The absorbance of Oil Red-O staining was measured using a plate reader at a wavelength of 560nm (n=6), Mean ± SEM. Mean absorbance values ± SEM (error bars) are shown. Statistical significance was determined using One-way ANOVA; P<0.0001. The stars represent the P value (ns P > 0.05), (* P ≤ 0.05), (**P ≤ 0.01), (*** P ≤ 0.001), (****P ≤ 0.0001)

Cells viability after treating them with IRCA drugs starting from the differentiation phase.

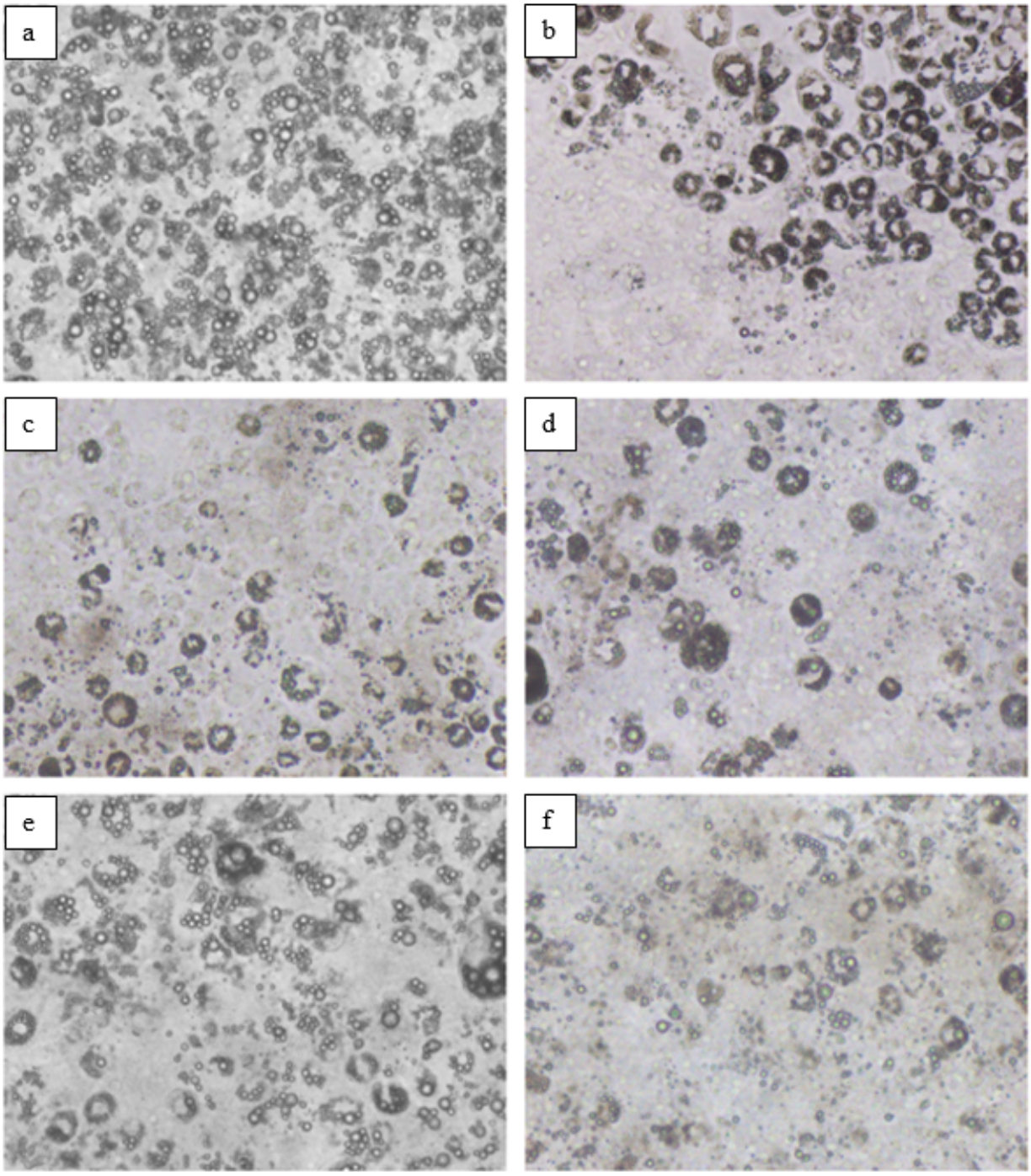

Figure 3. 9 cells viability After IRCA drugs treatment.

The cells were stained with Trypan Blue staining, then they were visualised under a light microscope. The image illustrates that all of the cells are alive, because clear cytoplasm present viable cells, whereas blue cytoplasm present nonviable cells. Treatments: (a) control (no drugs added), (b) IRCA1, (c) IRCA2, (d) IRCA3, (e) IRCA4, and (f) IRCA5.

3.3.3 Effect of IRCA drugs on adipose cells, differentiated from 3T3-L1 cells.

In this study, IRCA drugs were examined in adipose cells were differentiated from 3T3-L1 cells. At this stage, all of the cells contains fat droplets, which means that they were differentiated from pre adipose to adipocytes (Figure 3.10). (N=6 for each drug treatment).

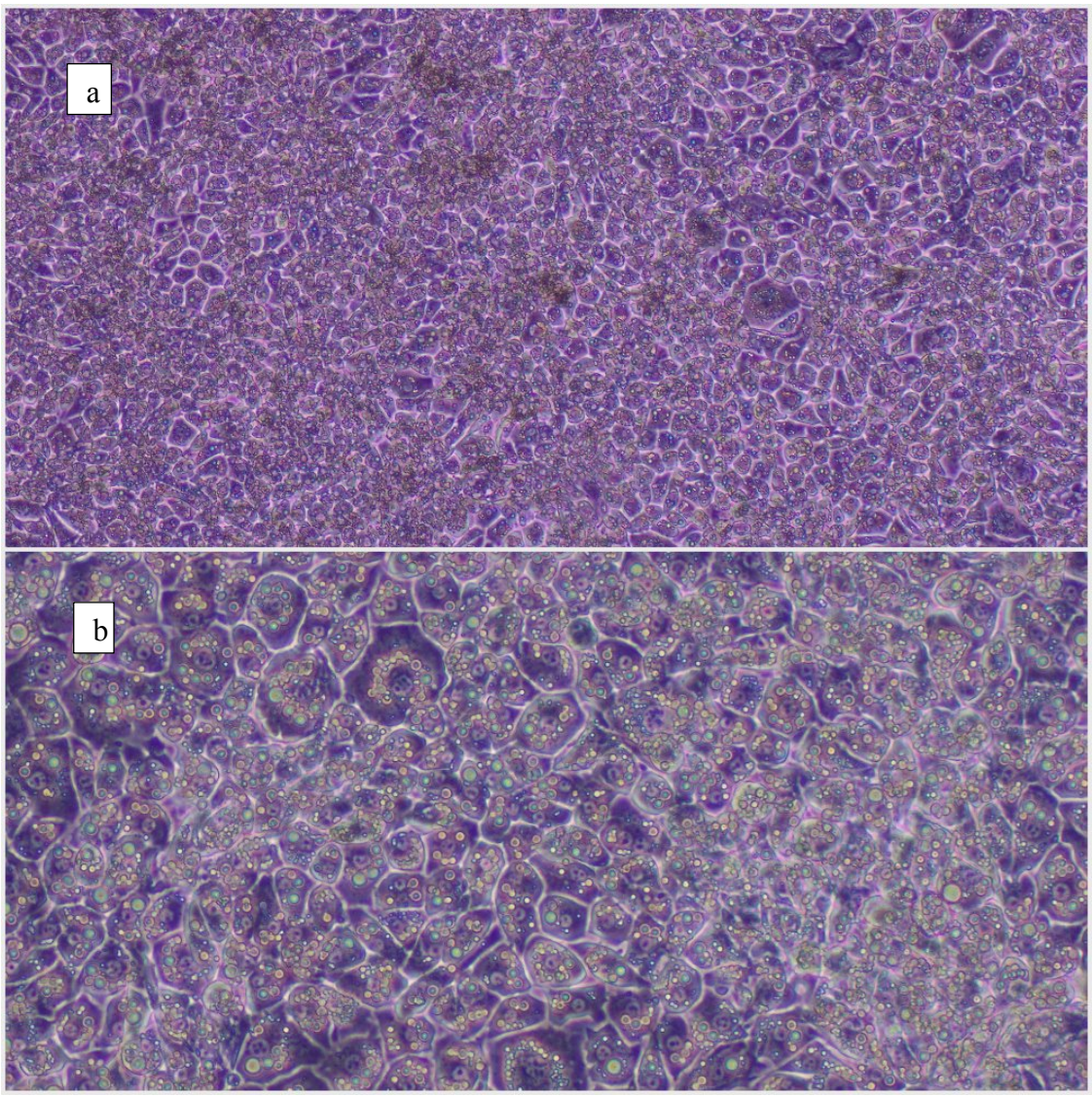

Figure 3.10 Adipose cells differentiated from 3T3-L1 cells

The cells were plated in a 6- well plate for 6 days. Then differentiation was for 3 days. Followed by post differentiation for another 3 days. 3T3-L1 cells are shown after differentiation, at 4x magnification x4 (a), and 10x magnification (b).

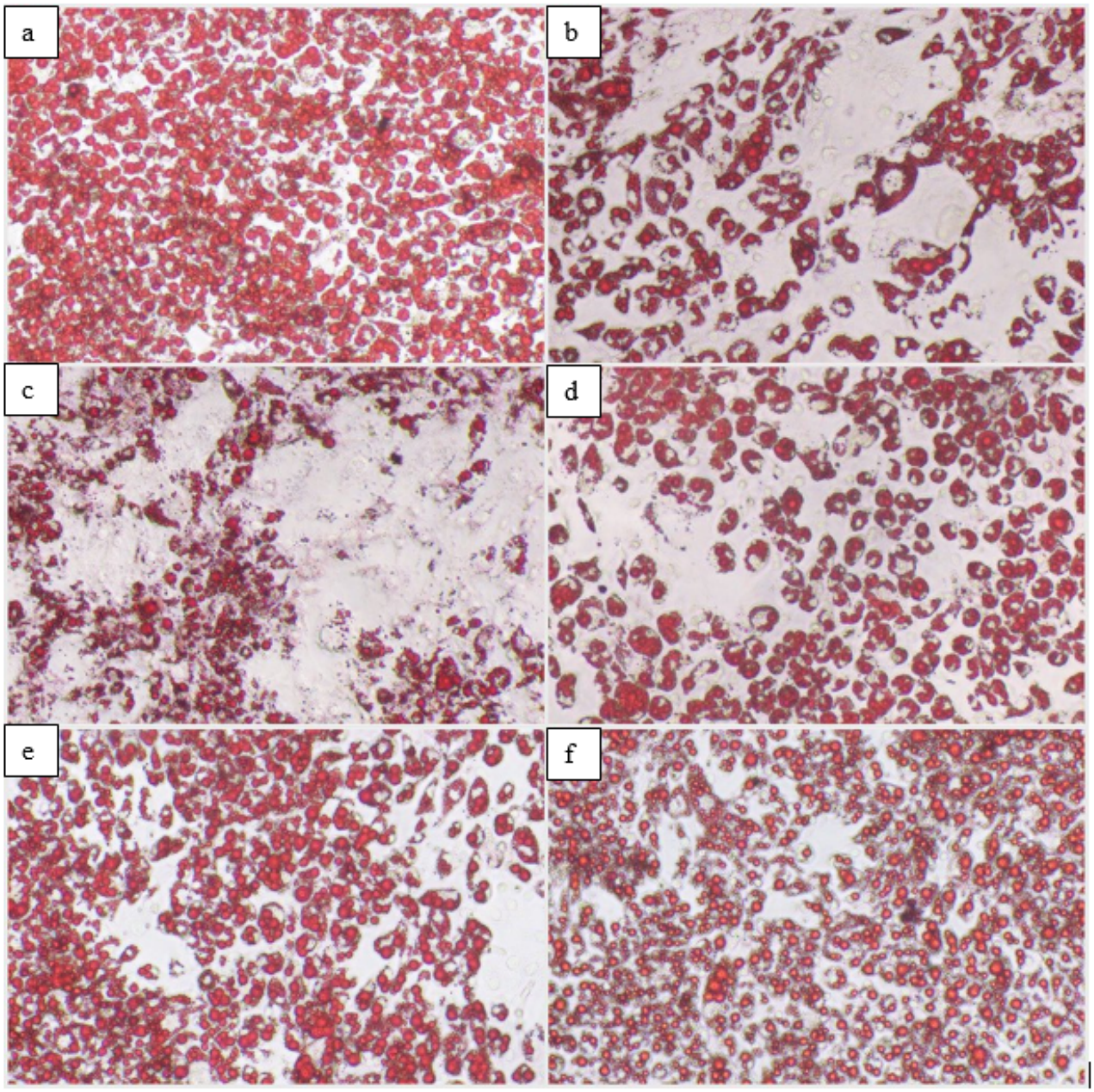

Figure 3.11 Effect of IRCA drugs on differentiated 3T3-L1 cells.

The cells were incubated with growth factors to promote differentiation, and incubated for three days. This was followed by incubation with post differentiation media for other three days. After that the cells were treated with IRCA drugs for 6 days. The cells were fixed with formalin. They were stained with Oil Red-O. the cells were visualised under a light microscope (10x magnification). (a) is the negative control, (b) is IRCA1showing less fat droplets compare to the control, (c) is the most effective drug IRCA2, with fewer and smaller fat droplets compared to the negative control, (d) the cells were treated with IRCA3, (e) the cells were treated with IRCA4, (f) the cells were treated with IRCA5.

Oil Red-O quantitation after treating 3T3-L1 with IRCA drugs After they had differentiated.

After the cells were stained with Oil Red-O, the stain was eluted using isopropanol. The absorbance of Oil Red-O was measured using a plate reader at a wavelength of 560nm.These drugs were reducing lipid content by the following percentages: IRCA1 (24.6%), IRCA2 (48%), IRCA3 (30.8%), IRCA4 (32%), and IRCA5 (34%). The data was analysed using One-way ANOVA test and the result was statically significants ($P < 0.05$).

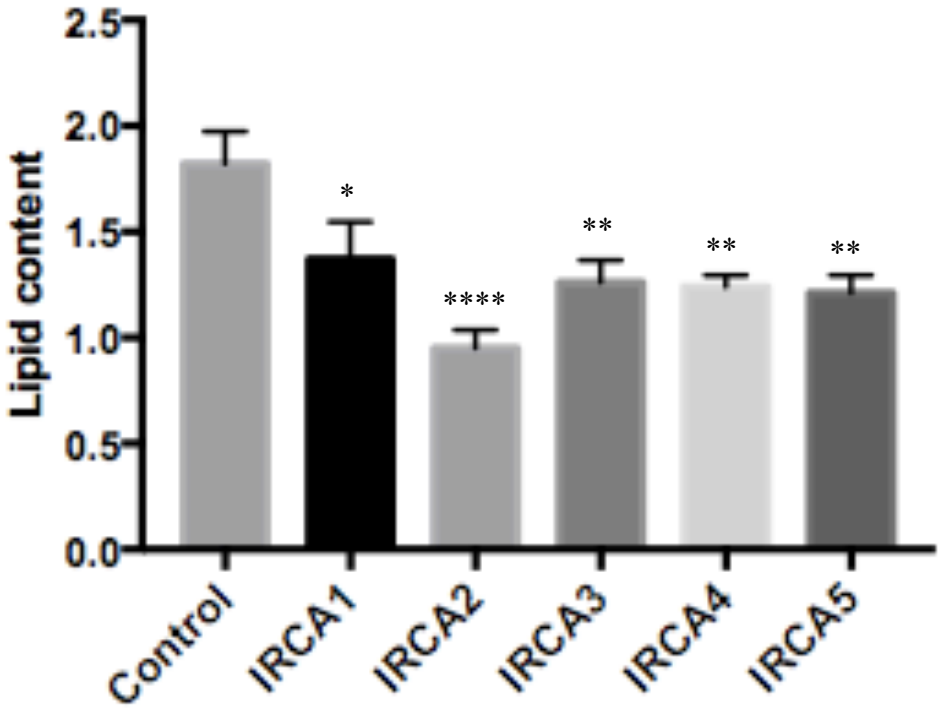

Figure 3.12 Effects of IRCA drugs on adipose cells

Effects of IRCA drugs on reducing lipid content from adipose cells, differentiated from 3T3-L1 cells. The absorbance of Oil Red-O staining was measured using plate reader 560nm (n=6).

IRCA drugs have significant effect on reversing fat droplets on differentiated 3T3-L1 cells after 6 days of treatment. The P value for the total experiment is 0.0006. The stars represent the P value (ns $P > 0.05$), (* $P \leq 0.05$), (**$P \leq 0.01$), (*** $P \leq 0.001$), (****$P \leq 0.0001$)

4. Discussion:

4.1 Expression of *Rcan1* in white adipose tissue in relation to age.

As mentioned earlier, *Rcan1* regulates obesity. One-year-old *Rcan1*$^{-/-}$ mice were protected from obesity after a normal fat diet compared to wild-type mice (unpublished data from our lab). As age is considered to be one of the risk factors of obesity, we decided to test whether the expression of *Rcan1* and its two isoforms *Rcan1.1* and *Rcan1.4* increase in white adipose tissue from wild type mice across different ages. *Rcan1* contains 7 exons and 6 introns (Figure 4.1). Rcan1.1 results from the splicing of exon 1 to exons 5 through 7 and *Rcan1.4* results from the splicing together of exons 4 through 7 (Figure 4.2).

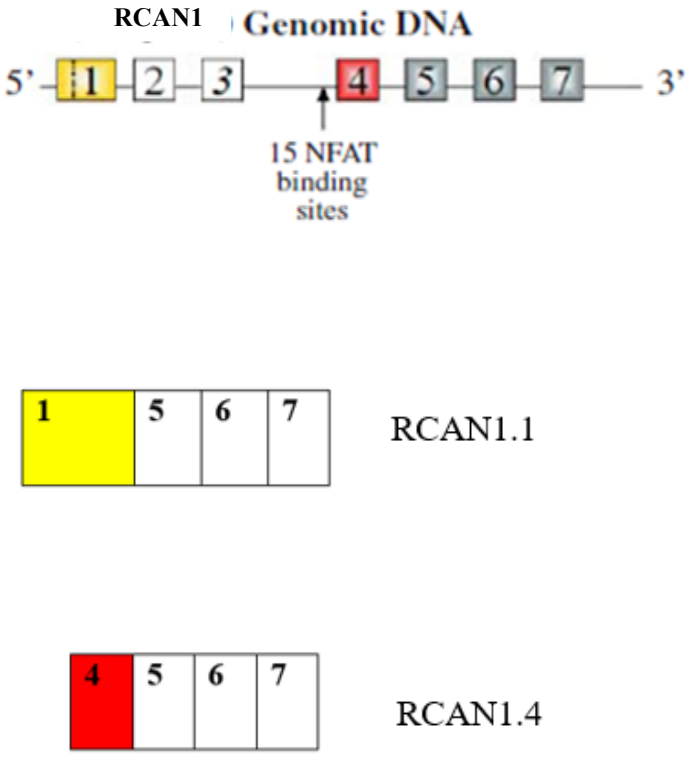

Figure 4.1 *RCAN1* Structure.

RCAN1 has seven different exons.

Structure of RCAN1.1 and RCAN1.4 protein isoforms.

Illustrates the main isoforms of RCAN1, which are RCAN1.1 and RCAN1.4

Four different ages were examined in our experiments, which are 6, 12, 18, and 24 months. There was no significant difference in the expression of *Rcan1*, *Rcan1.1,* or *Rcan1.4* across different ages in wild-type mice. The expression of *Rcan1.4* was more variable across the ages compared to *Rcan1.1* and *Rcan1*, which may have been partly due to *Rcan1.4* expression being approximately ten times less than *Rcan1.1*.

Given that *Rcan1* gene expression does not significantly change across different ages in wild-type mice, we can conclude that the loss of body weight in one-year-old wild-type mice (unpublished data from our lab) is not due to a decrease in *Rcan1* expression due to age. Weight loss in one-year-old wild-type mice is likely due to other factors. On the other hand, a lack of *Rcan1* expression in HFD mice results in less obesity despite the *Rcan1*$^{-/-}$ mice being housed in cages without exercise and being provided as much food as they want to eat. After one year of such a condition, mice will be more obese than they otherwise would be in nature. Therefore, under these obesogenic conditions, *Rcan1*$^{-/-}$ decrease obesity.

4.2 Expression of *Rcan1* in white adipose tissue in relation to diet.

Based on a previous study from our lab (unpublished data), which shows that *Rcan1*$^{-/-}$ mice are protected from obesity compared to wild-type mice under conditions of a high fat diet, we decided to examine *Rcan1* expression and its main two isoforms *Rcan1.1* and *Rcan1.4* in white adipose tissue of wild-type mice after a high fat diet and compare it with a low fat diet in the same tissue. While the result did not reach statistical significance potentially due to being underpowered because of limited dataset, the expression of *Rcan1*, and *Rcan1.1* trended higher in white adipose tissue after a high fat diet compared to a low fat diet. However, a higher *Rcan1* expression does not explain whether *Rcan1* expression causes obesity or whether factors related to obesity induce *Rcan1* expression. There might be several factors which may increase *Rcan1* expression, such as oxidative

stress, calcium, NFAT, and calcineurin (Peiris et al., 2012, Peiris et al., 2014), which may result in obesity.

4.3 Thermogenesis gene expression in white adipose tissue after a high fat diet.

A recent study from our collaborator, Dr. Beverly Rothermel, indicates that *Ucp1* expression increases in *Rcan1*$^{-/-}$ tissue after a 65% high fat diet for both 25 weeks and after a 60% high fat diet for 8 weeks (unpublished results). Therefore, in this study we examined the expression of genes related to thermogenesis after a 35% high fat diet which for 8 weeks, to see if a lower level of fat in the diet could still induce thermogenesis gene expression. Based on Dr. Rothermel's study, thermogenesis gene expression was expected to increase in *Rcan1*$^{-/-}$ white adipose tissue compared to the wild type tissue. However, the expression of the 6 thermogenesis-related genes analysed in this study (*Ucp1*, *Pgc1α*, *Pparγ2*, *Tnf-α*, *Mcp1* and *Cpt1α*) did not change in *Rcan1*$^{-/-}$ tissue. However, 5 of the genes did trend lower in expression in the knockout mice. This thermogenesis gene expression effect is different than the study by Dr. Rothermel, but the phenotypic change was similar, in that *Rcan1*$^{-/-}$ mice gained less weight than wild-type mice.

There might be several reasons for these unexpected results (ie no change in thermogenesis gene expression, but a general trend toward lower expression in knkockout mice). Firstly, the data from our experiments is underpowered, because of limited availability of mouse tissue. In addition, the result is not statistically significant. Another important reason might be that thermogenesis is actually unaffected in the 35% HFD mice for 8 weeks compared to mice given a 60% or higher fat diet.

The lack of thermogenesis gene expression changes in our study correlates with our observation the thermogenesis is not switched on there was no browning of the white adipose tissue in the samples (conversion to beige adipose tissue). Thermogenesis in our body mainly occurs in brown and beige adipose tissue, not white adipose tissue. Further, *Rcan1* is not just expressed in white adipose tissue;

it expressed in many different tissues such as brain and skeletal muscle, so the loss of *Rcan1* expression in these other tissues could also affect body weight.

There might be several reasons for weight loss in the *Rcan1*$^{-/-}$ mice under a high fat diet.

So when *Rcan1* is knocked out in mice, it is knocked out in all of the places that *Rcan1* is expressed, it is not just in adipose tissue, which means that the weight loss is not only due to effect of white adipose tissue.

Skeletal muscle uses 20-30 % of our total ATP to deal with regulating body temperature and muscle contraction. In comparison, white adipose tissue uses 5% of this energy (Rolfe and Brown, 1997). Energy usage by skeletal muscle might be the reason for losing body weight, not the browning from white adipose tissue. Therefore, this data suggests skeletal muscle was the cause of weight. The thermogenesis is not switched on at 35% high fat diet.

4.4 Effect of the Inhibitors of RCAN1-Calcineurin association (IRCA) in 3T3-L1 cells.

Another unpublished study by Dr. Beverly Rothermel indicates that when *Rcan1* expression is knocked down in 3T3-L1 cells, they produce less lipid content. Calcineurin has been shown to regulate the ability of 3T3-L1 cells to differentiate into fat cells by inhibiting the expression of transcription factors of pro-adipogenic genes (Almendro et al., 2009). Therefore, we decided to inhibit RCAN1, the main regulator of calcineurin, in 3T3-L1 cells using inhibitors of RCAN1-Calcineurin association (IRCA) drugs.

The aim of this study was to test 5 recently identified IRCA drugs (B. Chan., 2007) on 3T3-L1 cells at three different stages of growth. We first tested the effect of the IRCA drugs on differentiation to see if these drugs could inhibit adipocyte differentiation by analysing the development of fat droplets. Second, we examined whether these drugs stop the cells from growing more fat droplets when the drugs were added at the post differentiation stage. Our last aim was to find out whether IRCA drugs reduce fat content when added to fully differentiated cells that already contain lipids.

Effect of IRCA drugs on fat content in 3T3-L1 cells.

As expected, all 5 IRCA drugs were effective at reducing lipid content during the differentiation and post-differentiation phases of 3T3-L1 cells (Figure 2.4, 2.5 and Figure 2.6). IRCA2 was the most effective drug; the fat droplets in IRCA2 are smaller compared to the control and other drugs. This may be due to its different structure. The effect of IRCA drugs were effective on the three different phases that we tested, which means that Rcan1 has a positive effect on accumulation of lipid on fat droplet. Therefore, the IRCA drugs inhibit lipid accumulation in fat droplets

For the final study, we wanted to test whether these drugs could reduce lipid storage fat droplets. As is shown in Figure 3.9, all of IRCA drugs reduced lipid content in the differentiated adipose cells. This result was expected, since they inhibit *Rcan1*, which regulates calcineurin, a known regulator of adipognic (Neal and Clipstone, 2002, Ahn et al., 2008).

The IRCA drugs were effective at inhibiting RCAN1, thus inhibiting the ability of RCAN1 to bind to calcineurin. A study done by Chan et al. (B. Chan., 2007) found that IRCA drugs inhibit RCAN1 directly without inhibiting calcineurin, blocking interaction between RCAN1 and calcineurin (B. Chan., 2007).

These drugs might be good treatment for mice, we can test them using small doses and inject them in mice to see if they have any effect on them. It is known that some genes are essential to life, and when these genes are knocked out in mice, they die. However, based on the study that was done in our lab, knocking out *Rcan1* in mice does not affect their viability, the mice were healthy and normal and they were not sick.

Based on this, we expect that if we treat mice with IRCA drugs that inhibit the function of RCAN1 we would not expect them to die or to be sick because mice that have no *Rcan1* expression were alive and healthy. There are pros and cons of targeting the RCAN1 protein. These drugs are targeting RCAN1, which has a role in regulating obesity, however, we know that is expressed in

many different tissues. If there is a disease that is targeting a certain tissue, it is good if the target gene is only expressed in that tissue, which means that we do not have to think about the side effects. However, RCAN1 is expressed in many tissues, which means that the drugs might affect different tissues but we would not expect that the mice would get sick. The knowledge that we have about these drugs is limited, however, we know just the chemistry of them.

Often when drugs get injected into the bloodstream some changes could occur to them for instance, the drugs do not work as they did *in vitro*. We need to test these drugs on mice because they might not function as RCAN1 inhibitors when they are injected. The chance of these drugs to have an effect on mice might be low. However, we have the chemical structure of them. So we can develop these drugs by changing the weak points in their structure. We can develop these drugs to a drug that is going to be stable inside the mice.

Conclusion:

Our study suggests that *Rcan1* expression is not affected by age in white adipose tissue.

Rcan1 expression shows a trend towards higher levels in high fat diet compared to a low fat diet in wild-type mice. Expression of genes involved in thermogenesis trend lower in white adipose tissue in RCAN1 knockout mice compared to wild-type mice

Due to the low sample numbers in this study, it would be important to increase the data set to improve the confidence in the data.

IRCA drugs inhibited RCAN1, resulting in lower lipid content in pre-adipose 3T3-L1 cells differentiated to adipose cells, regardless of the stage at which they were added.

RCAN1 may be a good target for prevention and treatment of obesity, since blocking its expression and ability to bind calcineurin was able to reduce body weight without affecting the health of the mice and adipose cells in this study.

However, it is not clear whether the IRCA drugs, which were effective on cells in this study, would be effective and safe in mice.

References

AHN, J., LEE, H., KIM, S., PARK, J. & HA, T. 2008. The anti-obesity effect of quercetin is mediated by the AMPK and MAPK signaling pathways. *Biochemical and biophysical research communications,* 373**,** 545-549.

ALBERTS, B., JOHNSON, A., LEWIS, J., RAFF, M. & ROBERTS, K. Garland Science. 2002. *Molecular biology of the cell*.

ALMENDRO, V., FUSTER, G., AMETLLER, E., COSTELLI, P., PILLA, F., BUSQUETS, S., FIGUERAS, M., ARGILES, J. M. & LOPEZ-SORIANO, F. J. 2009. Interleukin-15 increases calcineurin expression in 3T3-L1 cells: possible involvement on in vivo adipocyte differentiation. *International journal of molecular medicine,* 24**,** 453.

ASSOCIATION, A. D. 2006. Diagnosis and classification of diabetes mellitus. *Diabetes care,* 29**,** S43.

BARNETT, T. & KUMAR, S. 2009. *Obesity and diabetes*, John Wiley & Sons.

B. Chan, Functional Studies of the Calcineurin-DSCRl Complex, in Division of Medical Sciences. 2007, Harvard University.

CECCHINI, M., SASSI, F., LAUER, J. A., LEE, Y. Y., GUAJARDO-BARRON, V. & CHISHOLM, D. 2010. Tackling of unhealthy diets, physical inactivity, and obesity: health effects and cost-effectiveness. *The Lancet,* 376**,** 1775-1784.

CUMMINGS, D. E. & SCHWARTZ, M. W. 2003. Genetics and pathophysiology of human obesity. *Annual review of Medicine,* 54**,** 453-471.

FUENTES, J. J., GENESCÀ, L., KINGSBURY, T. J., CUNNINGHAM, K. W., PÉREZ-RIBA, M., ESTIVILL, X. & DE LA LUNA, S. 2000. DSCR1, overexpressed in Down syndrome, is an inhibitor of calcineurin-mediated signaling pathways. *Human molecular genetics,* 9**,** 1681-1690.

GREEN, H. & KEHINDE, O. 1974. Sublines of mouse 3T3 cells that accumulate lipid. *Cell,* 1**,** 113-116.

KEATING, D. J., DUBACH, D., ZANIN, M. P., YU, Y., MARTIN, K., ZHAO, Y.-F., CHEN, C., PORTA, S., ARBONÉS, M. L. & MITTAZ, L. 2008. DSCR1/RCAN1 regulates vesicle exocytosis and fusion pore kinetics: implications for Down syndrome and Alzheimer's disease. *Human molecular genetics,* 17**,** 1020-1030.

KELLER, M. P., CHOI, Y., WANG, P., DAVIS, D. B., RABAGLIA, M. E., OLER, A. T., STAPLETON, D. S., ARGMANN, C., SCHUELER, K. L. & EDWARDS, S. 2008. A gene expression network model of type 2 diabetes links cell cycle regulation in islets with diabetes susceptibility. *Genome research,* 18**,** 706-716.

LEE, H. J., KIM, Y. S., SATO, Y. & CHO, Y.-J. 2009. RCAN1-4 knockdown attenuates cell growth through the inhibition of Ras signaling. *FEBS letters,* 583**,** 2557-2564.

MARCHETTI, P., DOTTA, F., LAURO, D. & PURRELLO, F. 2008. An overview of pancreatic beta-cell defects in human type 2 diabetes: implications for treatment. *Regulatory peptides,* 146**,** 4-11.

NEAL, J. W. & CLIPSTONE, N. A. 2002. Calcineurin mediates the calcium-dependent inhibition of adipocyte differentiation in 3T3-L1 cells. *Journal of Biological Chemistry,* 277**,** 49776-49781.

PARKS, B. W., SALLAM, T., MEHRABIAN, M., PSYCHOGIOS, N., HUI, S. T., NORHEIM, F., CASTELLANI, L. W., RAU, C. D., PAN, C. & PHUN, J. 2015. Genetic architecture of insulin resistance in the mouse. *Cell metabolism,* 21**,** 334-346.

PEIRIS, H., DUBACH, D., JESSUP, C. F., UNTERWEGER, P., RAGHUPATHI, R., MUYDERMAN, H., ZANIN, M. P., MACKENZIE, K., PRITCHARD, M. A. & KEATING, D. J. 2014. RCAN1 regulates mitochondrial function and increases susceptibility to oxidative stress in mammalian cells. *Oxidative medicine and cellular longevity,* 2014.

PEIRIS, H., DUFFIELD, M. D., FADISTA, J., JESSUP, C. F., KASHMIR, V., GENDERS, A. J., MCGEE, S. L., MARTIN, A. M., SAIEDI, M. & MORTON, N. 2016. A Syntenic Cross Species Aneuploidy Genetic Screen Links RCAN1 Expression to β-Cell Mitochondrial Dysfunction in Type 2 Diabetes. *PLoS Genet,* 12**,** e1006033.

PEIRIS, H., RAGHUPATHI, R., JESSUP, C. F., ZANIN, M. P., MOHANASUNDARAM, D., MACKENZIE, K. D., CHATAWAY, T., CLARKE, J. N., BREALEY, J. & COATES, P. T. 2012. Increased expression of the glucose-responsive gene, RCAN1, causes hypoinsulinemia, β-cell dysfunction, and diabetes. *Endocrinology,* 153**,** 5212-5221.

PRENTKI, M. & NOLAN, C. J. 2006. Islet β cell failure in type 2 diabetes. *The Journal of clinical investigation,* 116**,** 1802-1812.

RABINOWITZ, D. & ZIERLER, K. L. 1962. Forearm metabolism in obesity and its response to intra-arterial insulin. Characterization of insulin resistance and evidence for adaptive hyperinsulinism. *Journal of Clinical Investigation,* 41**,** 2173.

RAHIER, J., GUIOT, Y., GOEBBELS, R., SEMPOUX, C. & HENQUIN, J.-C. 2008. Pancreatic β-cell mass in European subjects with type 2 diabetes. *Diabetes, Obesity and Metabolism,* 10**,** 32-42.

RAO, A., LUO, C. & HOGAN, P. G. 1997. Transcription factors of the NFAT family: regulation and function. *Annual review of immunology,* 15**,** 707-747.

ROLFE, D. & BROWN, G. C. 1997. Cellular energy utilization and molecular origin of standard metabolic rate in mammals. *Physiological reviews,* 77**,** 731-758.

SALTIEL, A. R. & KAHN, C. R. 2001. Insulin signalling and the regulation of glucose and lipid metabolism. *Nature,* 414**,** 799-806.

STROBER, W. 2001. Trypan blue exclusion test of cell viability. *Current protocols in immunology***,** A3. B. 1-A3. B. 3.

TORAC, E., GAMAN, L. & ATANASIU, V. 2014. The regulator of calcineurin (RCAN1) an important factor involved in atherosclerosis and cardiovascular diseases development. *Journal of medicine and life,* 7**,** 481.

VEGA, R. B., ROTHERMEL, B. A., WEINHEIMER, C. J., KOVACS, A., NASEEM, R., BASSEL-DUBY, R., WILLIAMS, R. & OLSON, E. N. 2003. Dual roles of modulatory calcineurin-interacting protein 1 in cardiac hypertrophy. *Proceedings of the National Academy of Sciences,* 100**,** 669-674.

WANG, Y. & BEYDOUN, M. A. 2007. The obesity epidemic in the United States—gender, age, socioeconomic, racial/ethnic, and geographic characteristics: a systematic review and meta-regression analysis. *Epidemiologic reviews,* 29**,** 6-28.

WHITEHEAD, J. P., SIMPSON, F., HILL, M. M., THOMAS, E. C., CONNOLLY, L. M., COLLART, F., SIMPSON, R. J. & JAMES, D. E. 2004. Insulin and Oleate Promote Translocation of Inosine-5′ Monophosphate Dehydrogenase to Lipid Bodies. *Traffic,* 5**,** 739-749.

WU, J., BOSTRÖM, P., SPARKS, L. M., YE, L., CHOI, J. H., GIANG, A.-H., KHANDEKAR, M., VIRTANEN, K. A., NUUTILA, P. & SCHAART, G. 2012. Beige adipocytes are a distinct type of thermogenic fat cell in mouse and human. *Cell,* 150**,** 366-376.

ZEBISCH, K., VOIGT, V., WABITSCH, M. & BRANDSCH, M. 2012. Protocol for effective differentiation of 3T3-L1 cells to adipocytes. *Analytical biochemistry,* 425**,** 88-90.

ZHAO, E., KELLER, M. P., RABAGLIA, M. E., OLER, A. T., STAPLETON, D. S., SCHUELER, K. L., NETO, E. C., MOON, J. Y., WANG, P. & WANG, I.-M. 2009. Obesity and genetics regulate microRNAs in islets, liver, and adipose of diabetic mice. *Mammalian Genome,* 20**,** 476-485.

World Health Organization. (2016). Diabetes, 20162016,. Retrieved from http://www.who.int/mediacentre/factsheets/fs312/en/